A ROENTGEN STEREOPHOTOGRAMMETRIC ANALYSIS SYSTEM FOR THE MEASUREMENT OF SUBSIDENCE OF THE FEMORAL COMPONENTS IN TOTAL HIP ARTHROPLASTY

By

Brenda Gold

Submitted to the University of Cape Town in partial fulfilment of the requirements for the degree of Master of Science in Biomedical Sciences.

August 1993

I, Brenda Gold hereby declare that the work on which this thesis is based is my original work (except where acknowledgements indicate otherwise) and that neither the whole work nor any part of it has been, is being or is to be submitted for another degree in this or any other University.

I empower the university to reproduce for the purpose of research either the whole or any portion of the contents in any manner whatsoever.

.....Signed.....

SIGNATURE

.....5/8/93.....

DATE

ABSTRACT

The failure of total hip replacements due to aseptic loosening of the implanted components, remains an obstacle to the overall success of the technique. Various methods have been developed in order to detect loose components, but few offer the facility of the accurate determination of the magnitude of the migration of the prostheses. Migrations of between 0.1 mm and 3 mm may lead to the eventual failure of a replacement. One method which does allow the measurement of movements of this magnitude is Roentgen Stereophotogrammetric Analysis (RSA).

RSA relies on the production of a stereo pair of x-rays and the analysis thereof in order to determine the spatial position of the implanted prosthesis. The analysis of the stereo pair requires the orientation of the subject on each of the x-rays to be the same, hence the traditional use of two x-ray sources exposing the patient simultaneously.

This study investigates a new RSA system for the detection and measurement of subsidence of femoral components in total hip arthroplasties. The system has combined x-ray stereophotogrammetry with close range stereophotogrammetry, using video cameras, to provide an alternative system to those requiring two x-ray tubes. The system described requires one x-ray source, two video cameras and a PC to determine the spatial positions of internal marker beads and reference points on the prosthesis. The video cameras allow the location of the subject on the two x-rays and through mathematical manipulation the subject may be artificially rotated into the same co-ordinate system for the two x-rays. Changes in the calculated distances between the beads and the reference points on successive x-rays indicate subsidence which may be measured.

The system was tested and analysed using dry bone specimens implanted with retrieved prosthetic components and thereafter implemented in the initial stages of on-going clinical trials. The evaluation of the procedure in the bone-specimens showed that the reference

points could be co-ordinated with an accuracy of 0.2 mm and that distances could be measured with an accuracy of 0.3-0.4 mm in three-dimensions. The system is therefore capable of measuring subsidence of prostheses of 0.3 mm.

It is believed that the system will be of great value to orthopaedic surgeons in clinical situations where two x-ray sources with simultaneous firing control are unavailable. The accuracies determined in this study indicate implementation in routine clinical practice will provide valuable information regarding the position of the prosthesis.

ACKNOWLEDGEMENTS

I would like to thank the following people for their contributions to this study:

Prof LA Adams for his guidance as co-supervisor, his assistance in solving the numerous implimentation problems and for his limitless enthusiasm regarding the success of the technique .

Mr A Spirakis for his motivation and guidance as co-supervisor and assistance in the clinical arrangements.

Prof ID Learmonth for his co-supervison and for implanting the beads and prostheses for the bone studies.

Mrs B van Geems for refining existing software and writing additional software as needed and assistancing in the implementation of the system.

Mrs S Monk and Mrs M Preston of the Radiography Department at Princess Alice Orthopaedic hospital (PAOH) for taking the x-rays.

Dr G Hussel for implanting the beads for the clinical trials.

Sr F Schreuder of PAOH for arranging the beads for implantation.

Mr J Ireland for building and refining the control frame and camera stand.

TABLE OF CONTENTS

LIST OF ILLUSTRATIONS

LIST OF TABLES

GLOSSARY

Acetabulum:	The socket portion of the hip joint
Anterior:	The front of the body
Arthroplasty:	Surgical procedure to make a moveable joint
Bone ingrowth:	Ingrowth of bone into the porous metal coatings of prosthetic components
Distal:	The point further away from the trunk
Femur:	The bone of the upper leg
Inferior:	The lower end of the body
In vitro:	In the laboratory
In vivo:	In living bodies
Lateral:	Away from the midline of the body
Medial:	Towards the midline of the body
Necrosis:	The death of cells or tissue
Normal:	Perpendicular to
Osteoblasts:	Cells involved in the laying down of new bone tissue
Osteoclasts:	Cells involved in the breaking down of bone tissue
PMMA:	Polymethlymethacrylate: an organic polymer cement with minimal adhesive or bonding properties
Posterior:	The rear side of the body
Prosthesis:	A device which replaces a portion of the body
Proximal:	Nearer the trunk
Resorption:	The removal of bone tissue by the osteoclasts
Rigid body motion:	The translation or rotation of the body as a whole
Superior:	The top of the body

CHAPTER 1
INTRODUCTION

The total replacement of arthritically damaged joints has become the accepted treatment for the pain and discomfort associated with this disease. Since the 1960s when Sir John Charnley introduced the concept of Low-Friction Arthroplasty (LFA) the orthopaedic surgeon has been presented with many types of prostheses manufactured from various materials in attempts to solve some of the problems arising with the use of this procedure.

Success rates for the total hip arthroplasty (THA) procedures are increasing constantly, with the elimination of pain and improved joint mobility being the initial criteria for success. It is that small, but neverthless significant, group of initial failures and time related failed THA's that are of the most interest.

Aseptic loosening of one or both components in THA is one of the major causes of failure (Beckenbaugh and Ilstrup 1978, Cotterill *et al.* 1982, Cupic 1979, Gruen *et al.* 1979, Harris *et al.* 1982, McBeath and Foltz 1979, Pellicci *et al.* 1979, Stauffer 1982, Sutherland *et al.* 1982). Loosening of the femoral component is the more frequent complication in early follow-up studies (Harris *et al.* 1982, Munuera & Garcia-Cimbrelo 1990, Morscher 1983, Stauffer 1982, Sutherland *et al.* 1982). The initiation of femoral component loosening is primarily due to mechanical failures at the cement-bone interface which, in time, may cause fragmentation of the cement mantle and lead to bone lysis and, ultimately, loosening (Jasty *et al.* 1991). Once loosening is initiated additional factors such as the formation of soft tissue at the cement-bone interface (Goldring *et al.* 1983, Willert *et al.* 1974) and increased mechanical stresses in the cement (Jasty *et al.* 1991) escalate the problem.

Movement of the component in the femoral canal has been termed migration due to the small dimensions of that motion (Mjöberg *et al.* 1985). Subsidence is the specific migration of the component downwards into the femoral canal. A subsidence of approximately 0.5 mm in the first year is accepted as normal but, any further subsidence can precede failure of the THR (Freiberger 1986, Mjöberg 1986). Early detection of this subsidence would assist the surgeon in monitoring the cases with a high risk of failure and possibly intervening before the secondary effects of the loosening cause irreparable damage.

The diagnosis of loosening is based on the detection of continuous, progressive radiolucent lines on routine clinical follow-ups and/or pain experienced by the patient (Patterson *et al.* 1986, Schneider *et al.* 1982, Stauffer 1982). This, however, occurs when the loosening is at an advanced stage.

The magnitude of the micromotion is so small (0.1 mm-3 mm) that it is of utmost importance that the technique used to measure this movement be very accurate. Methods have been established to attempt to manipulate conventional roentgenographs (x-rays) in order to take measurements (Amstutz *et al.* 1986, Mulroy *et al.* 1991), but the accurate realignment of the patients in follow up observations, and the translation of the two-dimensional measurement into a three-dimensional one are associated problems. Arthography, scintigraphy, computed axial tomography (CAT), magnetic resonance imaging (MRI), ultrasound and acoustic vibration analysis have all been employed in attempts to detect migration (Turner-Smith 1990). These methods are able to detect movement, but, all have inherent problems and are not reliable as accurate measuring techniques and thus the extent of the loosening is not known.

A method which is proving to be reliable in the detection of these micromotions is Roentgen Stereophotogrammetric Analysis (RSA). The implementation of RSA requires a set of reference markers to be positioned around the implanted component, and a stereo-pair

of x-rays films to be exposed simultaneously. The stereo-pair allows the determination of the co-ordinates of the implanted markers and thus, their spatial positions with respect to prosthesis may be determined. It is the movement of the prosthesis with respect to these markers which indicates the magnitude and direction of any migration which may have taken place.

The aim of this study was to develop a RSA system to detect and measure subsidence of the femoral components in THA.

Our specific objectives were to: i) combine a single x-ray and a close-range stereophotogrammetric system, ii) undertake *in-vitro* experiments using implanted cadaveric femora in order to determine the accuracy, the repeatability and the validity of the methodology, iii) develop the "hardware" to be used in a clinical setting and iv) test the performance of the system when used with patients having undergone total hip joint replacement.

It was beyond the purpose of this study to undertake long-term follow-ups of these patients.

CHAPTER 2
ASEPTIC LOOSENING AND PROSTHESIS MIGRATION

2.1 CLINICAL BACKGROUND

The acceptance of total hip arthroplasty (THA) as the most successful treatment of arthritically damaged joints has prompted a great deal of clinical and biomedical research

The introduction of Sir John Charnley's LFA, i.e. a metal femoral component together with a small diameter head articulating with an acetabular component of ultra high molecular weight polyethylene (UHMWPE), and the introduction of polymethylmethacrylate (PMMA) bone cement saw a remarkable improvement in the success of THA.

As the designs and surgical procedures involved in THA's improved so too did the success rates increase. Figures as high as 90% have been quoted for the immediate success rate of eliminating pain and improving the overall functioning of the affected joint (Beckenbaugh and Ilstrup 1978, Charnley and Cupic 1973, Dall *et al.* 1992, Johnston and Crownshield 1983, Learmonth *et al.* 1991, McCoy *et al.* 1983, Melhoff and Sledge 1990, Wroblewski 1986). This impressively high figure does however, decrease with time and when dealing with younger patients (Learmonth *et al.* 1989). One of the major contributing factors in the long-term increase in the failure rates is aseptic loosening of the components (Beckenbaugh and Ilstrup 1978, Cotterill *et al.* 1982, Cupic 1979, Gruen *et al.* 1979, McBeath and Foltz 1979, Pellicci et al. 1979, Stauffer 1982, Sutherland *et al.* 1982). In long-term studies, figures of up to 62% of patients requiring revision THA's had loose prostheses without infection (Freiberger 1986, Jasty *et al.* 1991).

The initial mechanical destabilising effects occurring in the cement-bone interface begin a chain reaction in the surrounding tissue.

Living bone displays a continuous process of structural change throughout the life-span of an individual. Initially to achieve the genetically determined shape of the bone, proceeding through the developing stages to achieve the predetermined length and thickness and ultimately to maintain the shape and size through adult life and also to heal fractures and other injuries inflicted on the bone. These processes are characterised by the removal and deposition of bone in specific areas (Sevitt 1981). The removal of bone tissue, or resorption, is the process by which old or necrosed bone is removed under the action of specific bone cells called osteoclasts (Fowles 1985, Sevitt 1981). In opposition to the resorption of the bone, deposition of new bone takes place. Deposition of bone occurs through the action of another specific bone cell, the osteoblast, which initiate the formation of the hard mineralised tissue (Fowles 1985).

The genetically determined shape and external structure of bone may be influenced by the mechanical forces acting on the bone (Wolff 1892 in Sevitt 1981). Loads up to three times that of body weight are applied to the hip joint during normal daily activities (Davy *et al.* 1988). These loads are applied through the joint itself and through the muscles acting across the joint (Poss *et al.* 1988).

Immediately post-operatively, the bone around the surgical site begins to remodel. The regeneration of new bone forms the bone-ingrowth into porous coated devices and the mechanical interlocking with the irregular surfaces of bone cement (Poss *et al.* 1988). The formation of stromal elements characterize the initial stages of bone regeneration. The stromal elements establish a stabilizing framework to support the osteoblasts during their development stage (Ling 1988). Damage to the stromal elements at this stage may cause the regeneration process to be replaced by a tissue repair process, resulting in the soft tissue formation in the affected area, which further inhibit the bone formation.

The remodelling of the bone may adversely affect the immediate, stable fixation necessary for ultimate success of the THA (Morscher 1983, Pillar *et al.* 1986, Whiteside and Easley 1989). The initial mechanical interlocking of the implant and the bone is achieved by the surgeon at the time of surgery (Ling 1986). The surgeon ensures the component is securely seated, either by using polymethylmethacrylate (PMMA) cement or, by using the special design features on the cementless implants. The trauma associated with the preparation of the bone results in an area of necrosed bone around the implant due to mechanical, vascular and thermal damage (Ling 1986). The necrosis of the local vascular system is due to the reaming of the medullary canal (Slooff 1971, Rhinelander *et al.* 1979, Radin *et al.* 1982, Sund and Rosenqvist 1983). Thermal damage occurs due to the heat injury caused by the high heat of polymerization of the cement, and also by the toxic effects of the monomer in the cement (Willert *et al.* 1974, Feith 1975, Huiskes 1980, Mjöberg 1984).

The application of small loads to the joint, immediately post-operatively, may translate into relatively high stress concentration in the supporting bone (Poss *et al.* 1988). These loads may lead to fatigue failure of the dead bone in addition to disrupting the stromal elements in the new bone (Ling 1986, Poss *et al.* 1988). These disruptions may permanently compromise the stable fixation of the implant also, the remodelling of the bone as a result of the loads exerted by the muscle and the metal prosthesis, may lead to bone resorption around the implant resulting in the loss of initial stability and fixation.

Mjöberg (1986) examined the problem of prosthesis loosening and defined loosening as migration. It was shown that all loose prostheses migrated and that no non-migrating prostheses were loose, and that all components migrated rapidly for a period of four months post-operatively, after which slower migration was observed. The initial migration has been explained by the resorption of the necrotic bone adjacent to the prosthesis. Once the initial resorption has taken place the component is separated from the bone by a fibrous connective tissue layer resulting from the body's tissue repair processes (Goldring *et al.*

1983, Johanson *et al.* 1987, Lennox *et al.* 1987, Linder *et al.* 1983, Willert *et al.* 1974). The macrophages present in the fibrous membrane then resorb bone when they are stimulated by micromotions of the femoral component (Willert *et al.* 1974, Linder *et al.* 1983, Feith 1975).

Once migration has been initiated the possibilities of failure are increased as the bone is continually resorbed due to the continuous micromotions of the prosthesis (Paterson *et al.* 1986, Linder *et al.* 1983). Thus, the small initial micromotions lead to larger migrations and thus more pronounced loosening. The migration in some cases may be slow and remain undetected, both by the patient in the form of discomfort and pain, and by the surgeon from radiographs and function tests. In the remaining situations the migration continues and is soon detected by both patient and surgeon. Factors separating these two groups are age, sex, activities and reasons for the arthroplasty. For example, Gudmundsson (1985), reported incidence of loosening in males over the age of 60 as being four times greater than for females in the same age group, and Radiographic evidence of loosening in 57% of patients under the age of 35 have been reported (Learmonth *et al.* 1991).

The problem of micromotion, or migration, in the femoral component is thus a very real problem which affects approximately 10% of all total hip arthroplasty patients (Beckenbaugh and Ilstrup 1978, Charnley and Cupic 1973, Stauffer 1982, Rothman and Cohn 1990). If the bone resorption, and thus migration, continues until failure of the implant, valuable bone stock is lost which makes revision surgery that much more difficult. Another consideration is that those asymptomatic patients who may show signs of migration without experiencing pain may experience sudden catastrophic failures (Chafetz *et al.* 1984). The majority of researchers agree that an accurate method of detecting and measuring migration in the early stages is needed (Turner-Smith *et al.* 1990, Brand *et al.* 1986).

Brand (1986) identifies six reasons for early detection:

i) the general results give an indication as to the suitability of the particular procedure or prosthesis;

ii) identifying the incidence of loosening will provide information about "risk" factors in specific patients, for example. age, sex, weight, etc.;

iii) the rates of loosening give indications as to the appropriateness of total hip reconstructions;

iv) identifying the asymptomatic patients timeously can reduce the problems of sudden failure;

v) guidelines can be established to assist the surgeon in deciding when to perform a revision THA;

vi) early detection and measurement can provide an insight into the mechanisms of loosening and possible ways of preventing the problem.

The majority of reported results of loosening are founded on the basis of radiographic and clinical indications. The clinical definition is based on the incidence of painful hips and the radiographic definition due to the presence of continuous and progressive radiolucent lines around the prosthesis. Brand (1986) states that there is no universal definition of loosening according to the radiographic lines, and the judgement relies on the surgeon's interpretation of the radiographs in terms of the accepted definition of loosening for that institution.

Examples of clinical interpretations of loosening are:

Stauffer (1982): i) any cement/prosthesis lucency

ii) complete bone/cement lucency

iii) any position change

McBeath (1979): i) any femoral position change

Cotterill (1982): i) any progressive lucency

Gruen (1979): i) any progressive lucency

ii) any position change

iii) any cement fracture.

Learmonth *et al.*(1991) i) diffuse femoral bone-cement demarcation of 3 mm or more

Dall *et al.*(1992) i) three or more zones of >3 mm width together with

a) subsidence of >3mm at bone\cement interface;

b) subsidence of >5mm at stem\cement interface;

c) cortical thinning in three or more zones

From the above definitions it is clear that the need for a reliable technique, with predetermined definitions, is required to assist surgeons in determining the potential outcome of total hip arthroplasties.

2.2 METHODS EMPLOYED TO DETECT SUBSIDENCE

The methods used to detect subsidence in THA's discussed in this section are:

i) vibration analysis

ii) contrast and radionuclide arthography

iii) scintigraphy

iv) radiography and

v) roentgen (x-ray) stereo photogrammetric analysis (RSA).

2.2.1 VIBRATION ANALYSIS

The application of a vibration of known frequency to the knee and the measurement of the vibrations at the hip was reported by Rosenstein *et al.* (1989). It was noted that a sound hip produced pure, clear signals, whereas the signal from a patient with a loose prosthesis produced distorted signals due to the prosthesis rattling in the bone. Kerr *et al.* (1991) reported that an investigation into the effectiveness of vibration analysis indicated this technique could provide additional information as to the stability of the prosthesis to supplement standard x-ray investigations.

2.2.2 ARTHOGRAPHY

Contrast and radionuclide arthography require an injection of a contrast medium into the joint capsule followed by the exposing of one or two x-rays (Uri *et al.* 1984, Murray and Rodrigo 1975). The penetration of the contrast medium between the bone and the cement indicates the possibility of loosening (Salvati *et al.* 1971). It has, however, been shown by Murray and Rodrigo (1975) that a number of asymptomatic patients do show positive

arthrograms. O'Neill and Harris (1984) related the penetration of the contrast medium into the bone-cement interface as being analogous to the radiolucent zone in a conventional x-ray, which does not prove loosening. The extent of the penetration may thus be used as an indication of loosening. The diagnostic criteria used by O'Neill and Harris (1984), to assess loosening in 61% of revised total hip replacements, was penetration of the contrast medium in to the bone-cement interface of two centimeter or more, or if the contrast medium reached the prosthesis-cement interface.

The contrast medium used for contrast arthography is commonly water-soluble iodine (Mjöberg *et al.* 1985, Murray and Rodrigo 1975). A radio-nuclide contrast medium of ^{99m}Tc- sulphur colloid diluted in saline (Abdel-Dayem *et al.* 1982) may be mixed with the iodine solution in order for scintigraphic registrations to be made (Mjöberg *et al.* 1988).

After the injection of the contrast media the patient is made to move around before anterior and lateral x-rays are exposed (Mjöberg *et al.* 1988, Murray and Rodrigo, 1975). The scintigraphic registrations are made on transparent films using a gamma camera (Mjöberg *et al.* 1988).

Reported correlations between the diagnoses from the arthrograms and the clinical findings at surgery differ considerably. Salvati *et al.* (1971) and O'Neill and Harris (1984), reported a good correlation, whereas Murray and Rodrigo (1975) found a poor correlation. Factors contributing to the differing opinions could be the dense fibrous tissue described by Charnley (1965) which fills the bone-cement interface, resulting in contrast media penetration in asymptomatic patients, as well as the "natural" settlement of the prosthesis within the cement mantle.

The lack of standardized diagnostic criteria and the inability to provide qualitative results limits the application of this technique to investigations combined with other investigation techniques (Gelman *et al.* 1978).

2.2.3 SCINTIGRAPHY

Scintigraphy involves the intravenous administration of a radio-nuclide bone labelling medium followed by tomographic scanning. An increase in the biochemical activity around the joint indicates loosening of the component or infection (Weiss *et al.* 1979).

The radio-isotopes commonly used in scintigraphy are technetium and gallium. A patient undergoing radio-nuclide scanning is given an intravenous injection of the substance three to four hours before scanning, in the case of technetium scanning (Gelman *et al.* 1978, Rushton *et al.* 1982, Weiss *et al.* 1979) and two days, in the case of gallium scanning (Mjöberg *et al.* 1985, Rushton *et al.* 1982).

Technetium scanning may indicate loosening of the components due to an increased focal uptake of the radio-isotopes around the prosthesis (Gelman *et al.* 1978, Rushton *et al.* 1982, Weiss *et al.* 1979). As infected loosening is not clearly distinguishable from aseptic loosening on technetium scans, gallium scans used in conjunction with the technetium scans may provide a more complete picture (Rushton *et al.* 1982). Gallium uptake is increased in infected areas as a result of the increased number of polymorphonuclear leukocytes due to the infection (Rushton *et al.* 1982, Weiner *et al.* 1981).

Scintigraphy has shown to indicate loosening with high sensitivity in the case of the femoral component, but visual evaluation is more difficult in the acetabular component (Gelman *et al.* 1978, Mjöberg *et al.* 1985).

2.2.4 RADIOGRAPHY

Conventional radiographs are generally the first step in the evaluation of total joint replacements, both for painful joints and for standard follow-up evaluations. Radiolucent lines at the prosthesis-cement, cement-bone or prosthesis-bone interface are the features used to identify a loose prosthesis (Brand *et al.* 1985).

These radiolucent lines elicit concern about the longevity of the prosthesis. The greater the extent of the lucency the more cause for concern that exists. All radiolucencies are thus considered potentially dangerous to the success of the arthroplasty and are thus reported for assessment (Johnston *et al.* 1990). Few standard parameters for radiographic assessment of loosening in femoral components of cementless arthroplasties exist (Jakim *et al.* 1989).

Gruen *et al.* (1979) described loosening of the cemented femoral component by delineating seven zones in the anterio-posterior view of the proximal femur (fig 2.1) and detailing the evidence of loosening in each of these zones. These zones have become known as the "Gruen" zones and are used as points of origin to describe the nature of the interfaces. Using the "Gruen" zones, standard evaluation procedures and criteria for the evaluation of radiographs may be devised.

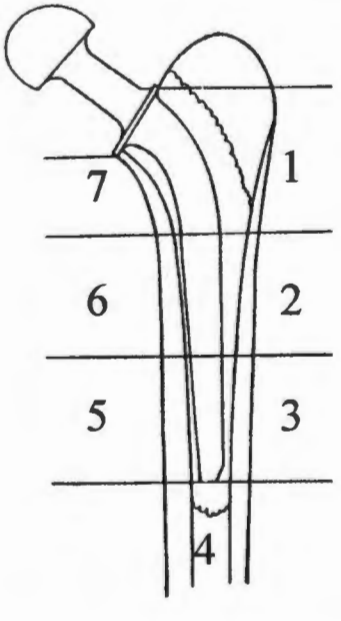

Figure 2.1 An illustration of the "Gruen Zones". (Adapted from Gruen *et al.* 1979).

Jakim *et al.* (1989), for example, described a six point system for the assessment of

loosening in uncemented prostheses.

These parameters are as follows:

1. Stem position: describing the angle between the femoral shaft and the prosthesis;

2. Stem contact in the femoral diaphysis: incorporating Gruen zones 2,3,5 and assessing the degree of contact of the bone and prosthesis in those regions;

3. Gruen zone 4: radio-opaque lines around the prosthesis tip;

4. Collar-calcar apposition: measuring the contact between the collar and the osteotomised end of the calcar;

5. Stem settling: recording the distance between the head of the prosthesis and the greater trochanter;

6. Adaptive bone remodelling: measuring the variations in the thickness of the cortical bone.

Radiographic evaluations using the Gruen zones do reveal signs of prosthesis loosening and subsidence in femoral components and in the case of patients with obvious pain and discomfort the cause is revealed instantly (Amstutz *et al.* 1986). However, merely indicating signs of migration and micromotion is not sufficient in the case of asymptomatic patients (Amstutz *et al.* 1986, Chafetz *et al.* 1984). The ability to compare successive radiographs in order to detect migration and subsidence and a need for quantitative evaluation directed attempts to standardise successive radiographs (Amstutz *et al.* 1986, Schneider *et al.* 1982). The primary difficulty in this standardization is the positioning of the patient in the same orientation in each successive radiograph.

Amstutz *et al.* (1986) introduced the technique of grid radiographs to ensure reproducible positioning of the hip and the x-ray beam. A Plexiglas sheet with engraved co-ordinates is

positioned over the patient and centered directly above the symphysis pubis. The x-ray tube is positioned directly over the femoral head and a radiograph taken with a lead marker positioned at the centre of the beam. The co-ordinates of the marker are kept on file for each patient in order to position the patient in exactly the same position for subsequent radiographs.

A method suggested by Mulroy *et al.* (1991), involves the insertion of a Herbert screw into the greater trochanter in the plane of the femoral component during surgery and the use of a component with a cylindrical extraction hole in the anterio-posterior direction. Before radiography the leg is manipulated until the extraction hole appears perfectly circular under fluoroscopic guidance. The circular hole and the Herbert screw thus act as reference points and any disparity between their positions on subsequent radiographs can be measured. This method is reported to be able to measure a migration of 1 mm with a high degree of accuracy (Mulroy *et al. 1991)*.

The introduction of computer technology as aids in the assessment of radiographs has further improved the standardization of the information obtained from the radiographs. Image analysis systems may be employed to measure numerous parameters from THR radiographs (Hardinge *et al.* 1991, Jones *et al.* 1988,1989). The system involves the transfer of the analogue radiographic image to a digital computer image. The image is transferred via a video camera, connected to a frame grabber card. The digital image is then stored on the computer and simultaneously displayed on a TV monitor. A mathematical filtering may be applied to unclear images to enhance the contrast (Hardinge *et al.* 1991). The computer generates reference points on the images using design features of the prostheses. These reference points are used to mathematically calibrate the successive radiographs. Hardinge *et al.* (1991) report that the reproducibility of the measurements being better than 0.01 mm with an accuracy of approximately 0.5 mm.

2.2.5 ROENTGEN STEREOPHOTOGRAMMETRIC ANALYSIS (RSA)

Radiographs provide two-dimensional (2-D) representations of three-dimensional (3-D) objects. As a result, measurements that are made, whether under standardized conditions or not, present mathematical problems (Hardinge *et al.* 1991). An extension of assessing single radiographs is to produce a stereo pair of radiographs and then to view and measure them stereoscopically to achieve a 3-D reconstructed image and thus a more realistic representation of the object. This procedure is known as Roentgen (x-ray) Stereophotogrammetric Analysis (RSA).

The procedure involves the implantation of metal beads into the bone surrounding the prosthesis during the initial surgical procedure. The beads serve as reference points for successive radiographs. Two radiographs are exposed from different orientations while the patient remains in the same position. A calibration system is used to calibrate the markers and the photographic film. The measurement of the reference markers and the calibration system is computerized and thus the successive radiographs may be mathematically manipulated to produce reconstructed images in the same orientations. This method thus provides the most accurate determination of position of a prosthesis and allows accurate measurements of any changes in that position to be computed (Baldurrson *et al.* 1979, Chafetz *et al.* 1984, Djerf *et al.* 1987, Green *et al.* 1982, Hunter *et al.* 1979, Lippert *et al.* 1982, Selvik *et al.* 1983, Turner-Smith *et al.* 1990, Veress *et al.* 1977). Using RSA it is possible to determine micromotion of the prosthesis of as little as 0.2 mm (Mjöberg 1986, Baldursson *et al.* 1979, Chafetz *et al.* 1984, Turner-Smith *et al.* 1990). The ability to measure such small micromotion is especially important in order to distinguish between the natural sinkage of approximately 0.5 mm during the first year and any larger migration which may be associated with premature failure of the implant (Mjöberg 1986).

CHAPTER 3
X-RAY STEREOPHOTOGRAMMETRY

Treatment of the skeletal system disorders relies on comparative observations and measurements of the affected area, for the duration of the treatment and for future follow-ups. The method of observation is required to be accurate and reproducible both quantitatively and qualitatively in order to detect the magnitude of changes in the order of 0.5-5 mm. Conventionally single x-rays are used. These single x-rays give the observer the opportunity of detecting small changes but do not allow accurate measurement as a result of the missing third dimension. The failure of the single x-ray to provide quantitative results in the orthopaedic practice paved the way for the development of x-ray stereophotogrammetry. X-ray stereophotogrammetry provides a 3-D, reconstructed, view of the object which allows measurements to be made. In order to determine the true dimensions of the object, two important criteria must be met: 1) that the orientation of the film with respect to a common coordinate system is known and that the reference points on the object be defined in terms of this coordinate system, and 2) that the position of the perspective centres of the two x-ray tubes also be known in terms of the common coordinate system (Brown *et al.* 1976).

To create stereo x-rays, two single x-ray exposures are made of the object in different orientations. Specific points on the x-ray pairs are then measured and a mathematical reconstruction of the system developed from which accurate measurements can be made.

3.1 X-RAY IMAGE FORMATION

The principles of x-ray stereophotogrammetry rely on the theories of the **central projection**. In brief this means that the details of the object being x-rayed are imaged on the x-ray film by means of rays, which originate from one point in space called the **perspective centre** (Hallert, 1970). The perspective centre in x-ray photogrammetry is the focus (focal spot) of the x-ray tube. In reality the focal spot of the x-ray tube has a finite size, but the perspective centre is assumed to be a single point (fig. 3.1).

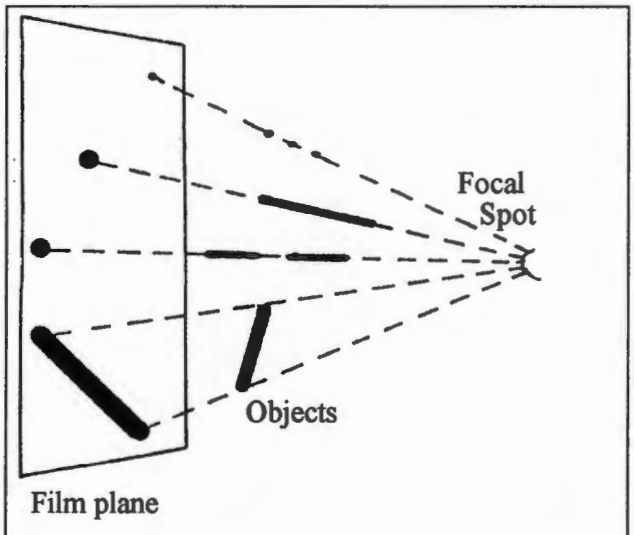

Figure 3.1. The relationship between the perspective centre, object and film. (Adapted from Hallert 1970)

The x-rays passing through the perspective centre are collectively called a bundle of x-rays. The x-ray bundles are produced by high speed collisions of electrons emitted from the cathode filament with the electrons in the anode target (fig.3.2). The collisions result in an energy transfer in the form of heat generation. Most x-ray tubes have a rotating anode which prevents overheating and allows higher voltages to be applied to the cathode, increasing

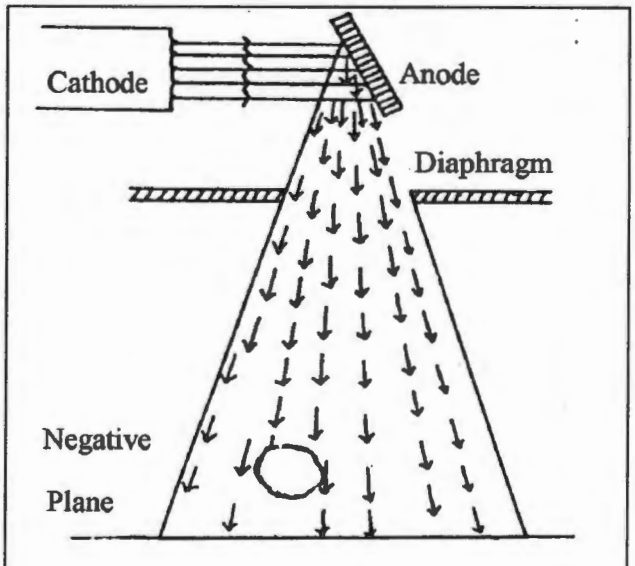

Figure 3.2. A schematic representation of an x-ray tube. (Adapted from Hallert 1970)

the formation rate of the x-ray bundles.

X-ray images are regarded as more or less dense shadows of the object (Hallert 1970). The differential x-ray absorption by the object forms the characteristic image on photographic film. A number of factors relating to the x-ray bundle generation, the object being imaged and the film used, affect the ultimate quality of the final x-ray image.

X-rays are highly penetrating, invisible rays which are electronically neutral and cannot be deflected by electric or magnetic fields or be focussed by optical means (Veress 1989). X-ray bundles travel in straight lines from the focus of the tube. Their passage through an object tends to cause the x-rays to scatter resulting in a poorly defined image on the film. To prevent this loss of definition a "Bucky" grid, consisting of parallel lead vanes converging on the focus of the x-ray tube, is placed in front of the film (fig.3.3). The direct rays are absorbed by the vanes and thereby reduce the diffusion. The vanes are not visible on the film as the "Bucky" moves rapidly back and forth across the film during an exposure.

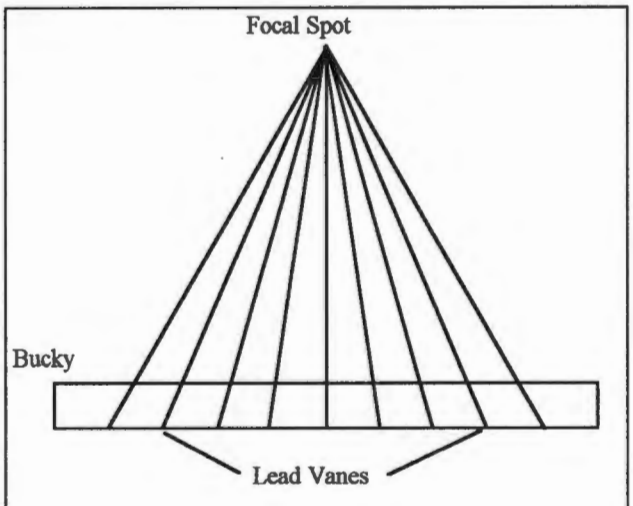

Figure 3.3. The lead vanes of the "Bucky" grid converging on the focal spot of the x-ray tube. (Adapted from Karara 1989)

The amount of current applied to the cathode, in order to produce the electrons, as well as the duration of the applied current (exposure time) determine the image density of the x-ray. The voltage gap between the cathode and the focus determine the image contrast. These factors are set by the radiographer and are determined by the image requirements and by the object to be imaged.

3.2 DEGRADATION OF X-RAY IMAGES

A certain degree of definition and clarity in x-rays is lost when living subjects are exposed. This is due to the adjustments needed to protect the patients from high doses of x-ray radiation.

There are methods of reducing the exposure time and exposure intensity when exposing patients. Reducing the exposure time and the concentration of the x-rays results in diffused, unclear images. Various methods of enhancing the ability of x-rays to produce clearer images on the x-ray film are employed in conjunction with the decreased exposure time and intensity. These methods include the choice of film and the introduction of intensifying screens.

Films are available with either a single or double emulsion. A single emulsion film has the x-ray and light sensitive chemical or emulsion on one side only, whereas double emulsion film has a coating of emulsion on both sides. A double emulsion film registers an image faster and requires less exposure than the single emulsion film. However, the double emulsion film causes a blurred effect on the film as the image is registered in both emulsions. Single emulsion films are thus used in x-raying non-living subjects. Double emulsion films are required to reduce the exposure time when dealing with patients. Enhancement of the exposure thus becomes necessary, and even critical. A cross section of a typical x-ray film cassette used when patients are to be x-rayed is shown in fig 3.4.

Further additions to the x-ray cassettes are the intensifying screens which shorten the exposure time. The screens have a coating of fluorescent crystals held in a lacquer, which emit a blue light when exposed to x-rays. The x-ray film is exposed by the blue light. Although the exposure time is reduced, the images on the film are formed by emitted light and not by direct x-rays and are thus not as clearly defined as a direct exposure image

would be. The exposure time without an intensifying screen would be approximately 25 times longer than with the screen (Karara 1989).

The third factor affecting the clarity and definition of the x-ray image is known as the penumbra effect. The penumbra effect is the softening or diffusion of the image edges due to the limited size of the focal spot of the x-ray tube, which is approximately 0.3 mm when patients are being x-rayed. This size allows the generation of sufficient x-rays to expose the film in a relatively short time. Reducing the focal size would decrease the penumbra effect, but the exposure would be too long to be safe for a patient. It was concluded by Veress (1989), that the errors caused were all positive and that the magnitudes of the errors were small enough to be negligible in practice as the image is larger than the object. No additional precautions are necessary to account for the penumbra effect.

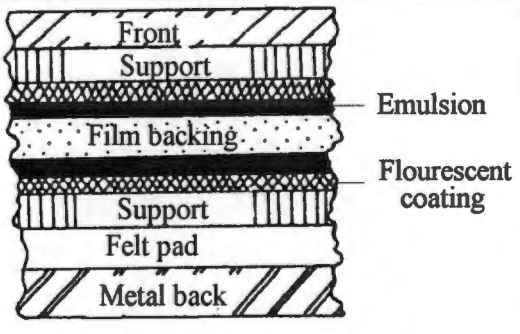

Figure 3.4 A cross section of a typical x-ray cassette. (Adapted from Karara 1989)

3.3. STEREO X-RAYS

In order to make measurements from x-rays, a 3-D view is required. To obtain this 3-D view a set of stereo pairs of x-rays are required. A stereo pair of x-rays is obtained by two x-ray films being exposed from two different perspective centres. The position of the object in space may be recreated by using a stereoscope to view the stereo pair and thereby obtain a visual representation or by measuring the 2-D coordinates of common points on the stereo pairs and mathematically determining the 3-D coordinates of that object (Adams 1981). The majority of stereo x-ray pairs analyzed in x-ray stereophotogrammetry are analyzed mathematically and therefore the base-distance ratio

need not be limited by the ability of the operator to comprehend the third dimension from the two x-rays on a stereoscope.

A stereo pair of x-rays can be obtained via a number of different equipment configurations. In the configuration shown in fig 3.5, two x-ray tubes are positioned a fixed distance apart. A single x-ray film is used and is exposed simultaneously by both x-ray tubes (Karara 1989). This set-up reduces the possibility of the patient being in different positions on the two x-rays. The major draw backs to this system are the costs and the availability of having two x-ray tubes and two power sources in one room.

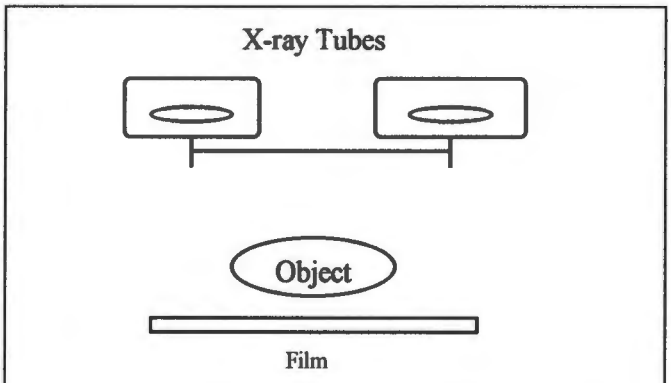

Figure 3.5. A schematic representation of the orientation of two x-ray tubes positioned a fixed distance apart used with a single film. (Adapted from Karara 1989)

A variation on this system is one in which the x-ray film and object remain stationary and a single x-ray tube is moved parallel to the film (fig 3.6). This system has the advantage of availability, as long as a mechanism is introduced for the parallel movement of the film (Karara 1989). The general unwieldiness of the x-ray tube in this system is a disadvantage as is the

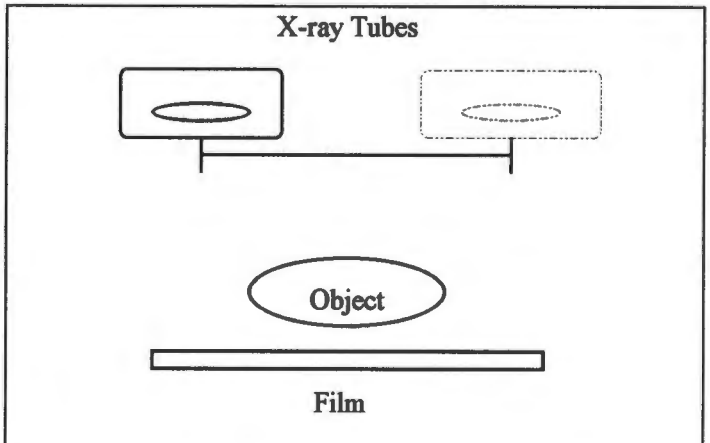

Figure 3.6. One x-ray tube moved a fixed fistance parallel to the film to obtain the stereo pair of x-rays. (Adapted from Karara 1989)

unsettling effect of the move on the patient who is required to remain still for the duration of the procedure.

A system which can be used when dealing with non-living, stationary objects is one in which the film cassette and the object are rotated while the x-ray tube remains stationary (fig 3.7). To apply this system in patients will result in errors to be accounted for, due to the possibility of patient movement in addition to the rotation.

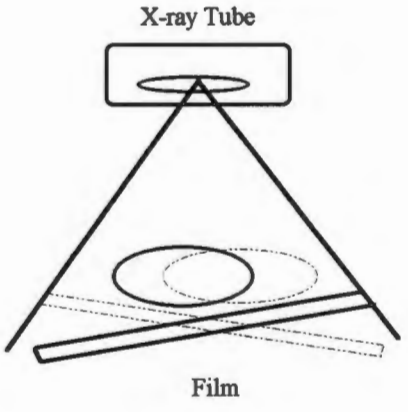

Figure 3.7. Stereo pairs of x-rays obtained by rotating the film and the object in front of a stationery x-ray source. (Adapted from Karara 1989).

A third system is one in which the film cassette and object are moved parallel to the x-ray tube (fig 3.8). The possibility of patients moving in this system may once again create a problem.

In all the above systems the calculation of the position of the points in space rely on the intersection of the x-rays from the two tubes. The smaller the angle between the intersecting rays, the less accurate the determination of the third dimension. This is illustrated in fig. 3.9, where the intersection is not a discrete point for the angle less than 90°. The

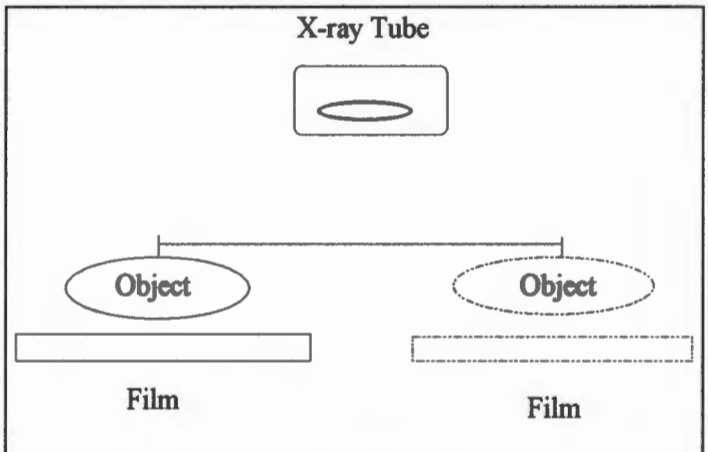

Figure 3.8. Geometry for obtaining stereo pairs by moving the film parallel to a stationery x-ray source. Adapted from Karara 1989.

most precise determination of the intersection point will thus result from a right angle intersection.

To achieve this, a system with the two x-ray tubes positioned at 90° to each other (fig 3.10) is used. This configuration also facilitates the simultaneous exposure of the two x-rays, which solves the problem of patient movement. The two x-ray films are placed perpendicular to each of the tubes which necessitates an adequate method of shielding to prevent the films being exposed to secondary radiation. The same disadvantages apply to this system as do for the first system described, namely cost and availability of the equipment.

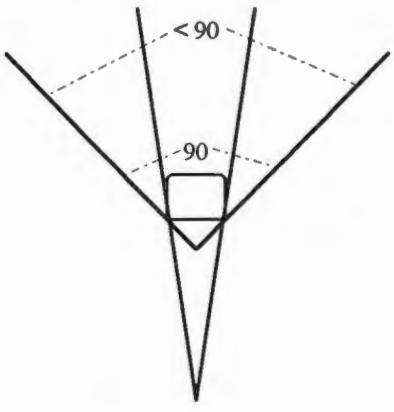

Figure 3.9. An illustration of the angles between intersecting rays to best determine the third dimension.

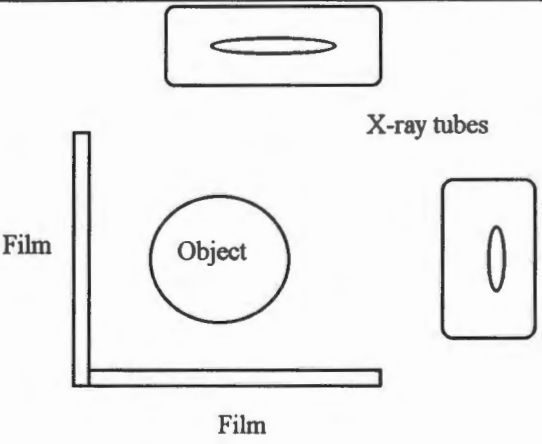

Figure 3.10. A geometric representation of the two x-ray tubes positioned at 90° to each other. (Adapted from Karara 1989)

3.4. CALIBRATION OF THE X-RAY SYSTEM

In order to make sensible measurements, the x-ray system used to obtain the stereo pair of x-rays is required to be calibrated in order to determine the interior orientation of the x-ray, or the relationship between the focal spot and the plane of the x-ray (fig. 3.11). This relationship is essential in the reconstruction of the x-rays forming the image. The elements required to determine the interior orientation are the **principle distance** i.e. the perpendicular distance from the focal spot to the film plane, and the position of the **principle point**, i.e. the foot of the normal from the film plane to the focal spot.

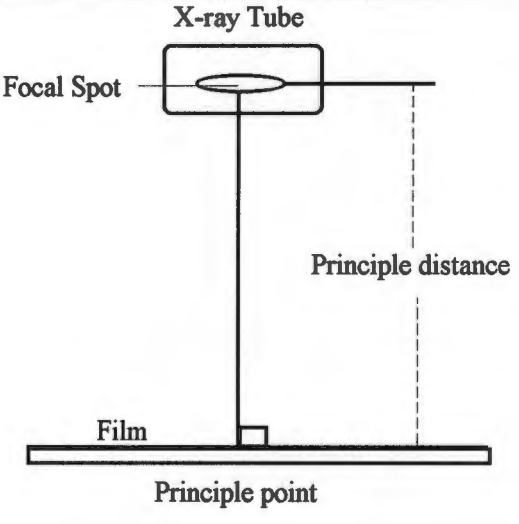

Figure 3.11. The relationship between the principle point and principle distance.

The principle point may be determined through physical, semi-analytical or totally analytical methods. Examples of physical calibration methods are described by McNeil (1966) and Jonason and Hindemarsh (1975).

Fig 3.12 is an illustration of the method used by McNeil. The system comprises a reference

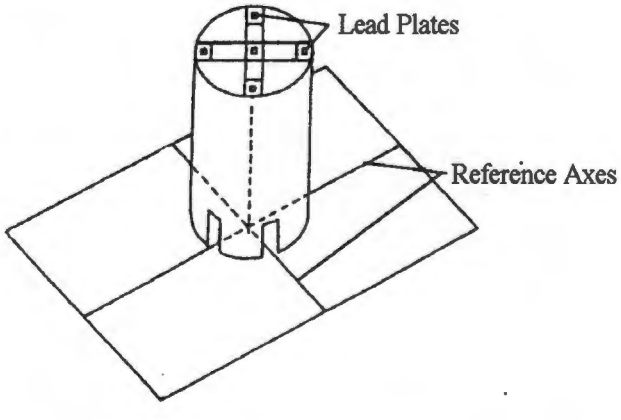

Figure 3.12. An illustration of the method used by McNeil to determine the principle point of the x-ray tube. (Adapted from Veress 1980)

plate with a radio-opaque system of axes imbedded in the plate. A right cylinder, containing five lead wafers in the upper face, is then positioned on the reference plate with the central axis of the cylinder on the origin of the axes. The lead wafers have tiny conical pinholes with the central pinhole lying on the axis of the cylinder. A test exposure indicates the magnitude and direction in which the focal spot has to be moved in order to make the principle spot coincident with the origin of the reference axes.

The calibration system (fig 3.13) used by Jonason and Hindemarsh consisted of two plexiglass sheets separated by metal rods. Embedded in the upper plate is a lead ring directly above a radio-opaque point in the lower plate. The point on the lower plate indicates the principle point when the ring is evenly around the point. If the point and the ring are not concentric in the test exposure the principle point can be determined by calculating the adjustments necessary to achieve this concentricity.

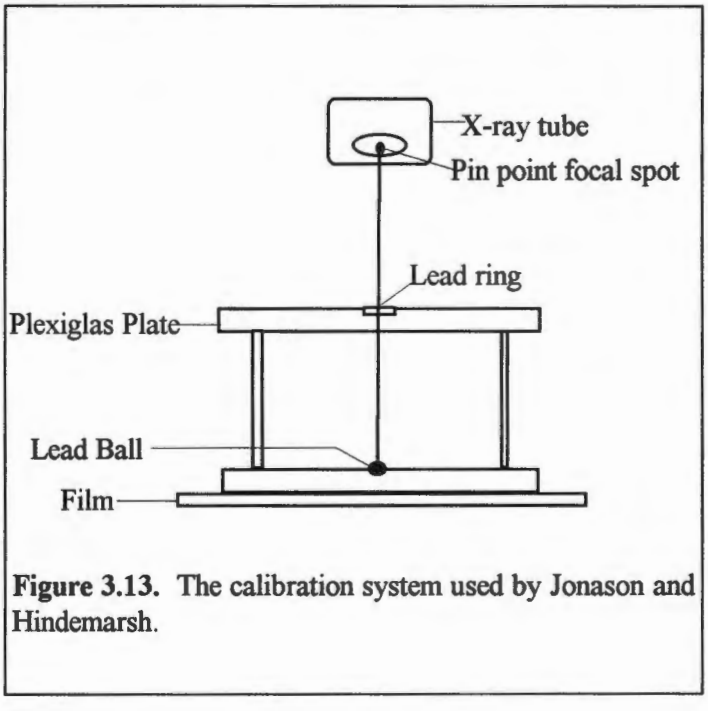

Figure 3.13. The calibration system used by Jonason and Hindemarsh.

The semi-analytical calibration methods described by Agnoletto and Pagani (1974), Moffit (1972) and Baumrind (1975) are based on the "plumb-line method". Agnoletto and Pagani's method relies on the film plane being strictly horizontal. Plumb points are marked on the film using conventional plumbing techniques and the intersections of the plumbing lines used to calculate the principle point. The method also relies on the precise location of the focal spot of the x-ray tube, which is often inaccessible. The principle distance is physically measured by measuring tape.

Moffit (1972) and Baumrind (1975) use the same plumbing techniques, but do not require the film plane to be perfectly horizontal. Four tubes with numbered radio-opaque markers on either end are positioned on each corner of a base plate (fig 3.14). On the film the lines joining the top and bottom markers of each tube are joined and extended to intersect each of the other lines. The principle point is then determined by applying a least squares solution. The principle distance is calculated from the measured geometry of the set-up and from the image distances of the radio-opaque markers appearing on the film.

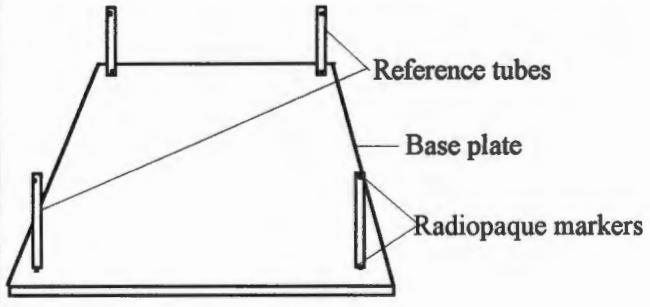

Figure 3.14. An illustration of the four corner tubes with embedded radio-opaque markers positioned on a base plate. (Adapted from Veress 1989)

A fully analytical method involves the co-ordination of control points and the mathematical derivation of the principle distance.

When rotating the tube discrepancies in the principal distance between the first and second positions do occur. These discrepancies need to be rectified or accounted for in any calculations in order to achieve a true 3-D determination.

A control system is used to ensure that the external conditions are the same for the two exposures in the stereo pair. The exterior control system consists of radio-opaque objects placed in the area of the object to be x-rayed. The precise 3-D co-ordinates of the points have to be known. These exterior control points can be either thin metal wires attached to a framework or metal beads imbedded in a plexiglass framework. The control points have to be positioned in such a way so as to ensure they are imaged on both x-ray exposures.

Internal object markers are essential, if precise dimensions and comparisons are required, to overcome the reduction of the image due to the degradation of the x-rays as discussed previously. This is particularly important in the case of patients due to the continual physiological changes surrounding a living skeletal system. The internal markers are usually metallic beads implanted into the area surrounding the prosthesis. The beads remain fixed in the bone and serve as reference points for all future x-rays.

3.5. MEASUREMENT OF THE STEREO X-RAYS

There are three basic methods of measuring the x-ray films to obtain quantitative results. The instruments used in these methods are: i) a stereo x-ray comparator; ii) a stereoplotter; iii) a PUG marker and a conventional digitizer and iv) an x-ray digitizer.

The stereo x-ray comparator used to measure stereo pairs of x-rays must have a measuring area large enough to accommodate both x-ray films. If this is not the case the x-rays are reduced by forming diapositives. The making of diapositives introduces additional precision problems, such as the differing latitudes of the diapositive emulsion and the x-ray film. Instruments such as the Zeiss STR-3 stereo x-ray comparator have a measurement field large enough to accommodate 40 x 40 cm x-rays thus alleviate the need for diapositives and have measuring capabilities up to 0.1 mm in the x and y planes (Veress 1989).

The use of a conventional photogrammetric stereoplotter requires the strict maintenance of geometry. This generally implies that the x-ray film be reduced to half its dimensions and the focal length of the plotter be set at half the principle distance of the x-ray. Diapositives are usually created to improve the contrast of the x-rays and to make stereoscopic vision easier. A further limitation with a conventional stereoplotter is the problem associated with the small base-height ratio required for the x-rays. The stereoplotters are seldom

used as a result of the difficulties in maintaining the strict geometry and the time required to make the diapositives.

A regular digitizer can be used in conjunction with a marking device such as a PUG marker. The PUG marker is used to zoom in on a point and then mark the point by cutting a hole into the emulsion of the film. The holes may be 20 to 120 micrometers in diameter (Veress 1989). The holes are then made more visible using a wax pencil and the points co-ordinated using a conventional digitising tablet.

A digitiser especially designed for use with x-rays has a lighting tablet built in. This illumination relieves the need to mark the film as the points of interest are visible due to the contrasts in the film. The digitising procedure is the same as for a conventional digitiser.

All the above described devices require the x-rays to be measured while being viewed stereoscopically. The instruments thus have to be large enough to accommodate the size of the x-ray films used. If this is not the case the films are reduced and the geometry of the system altered to fit the new size. These reductions and the making of diapositives are time consuming and require specialised personnel to operate the systems. The introduction of a micro-computer into the digitising phase makes it possible for the x-rays to be digitised separately and by using specialised software, the image may be reconstructed.

3.6. APPLICATIONS OF THE X-RAY STEREOPHOTOGRAMMETRIC SYSTEMS

Applications of x-ray stereophotogrammetry are wide spread in all spheres of measurement. One area of application is the determination of movement, migration and subsidence, of joint prostheses in the orthopaedic field. The migration of various types of

acetabular components in primary total hip arthroplasties has been measured (Snorrason and Kärrholm 1990, Mjöberg *et al.* 1986, Baldursson *et al.* 1980) as well as the subsidence in femoral components (Green *et al.* 1983, Wykman *et al.* 1988, Mjöberg *et al.* 1986, Chafetz *et al.* 1984). The measurement of micromotion of tibial components in total knee arthroplasty has also received attention from various groups (Green *et al.* 1983, Ryd 1986, Ryd and Toksvig-Larsen 1993, Nilsson *et al.* 1991, Walker and Sathasivam 1992). A number of these applications are reviewed in the following chapter. Spinal deformities such as the movements of the sacroiliac joints have been co-ordinated and are monitored during treatment using stereophotogrammetry (Jonason and Hindemarsh 1975, Kratky 1975, Brown *et al.* 1976, Sturesson *et al.*. 1989). A further orthopaedic application is the surface topography and the measurement of cartilage thickness in intact knee joints (Ateshian *et al.* 1991). Orthodontic interest in the structure of the jaw bone and teeth are also assisted by x-ray stereo photogrammetry.

CHAPTER 4
ROENTGEN STEREOPHOTOGRAMMETRIC ANALYSIS SYSTEMS

A number of roentgen stereophotogrammetric analysis (RSA) systems have been developed in various centres around the world to deal with measurement problems associated with orthopaedic surgery and more specifically with measurement after total joint replacements. This chapter will attempt to summarise the most important aspects of each of the better known, original RSA systems as well as their documented advantages and short comings. The systems have been named according to the centre in which they were developed and described from the respective researchers' published data and a review by Turner-Smith (1990).

Descriptions of the various RSA systems can be divided into the following areas: i) **clinical procedure:** preparation of the patient and the prosthetic components; ii) **x-ray procedure:** orientation of the x-ray tubes, films and patient; iii) **calibration:** methods used to determine the interior orientation of the system as described in the previous chapter; iv) **measurement:** techniques and instrumentation used to capture the necessary data and v) **analysis** of the data and presentation of the results.

4.1. THE OXFORD SYSTEM

The Oxford RSA system was developed by Turner-Smith *et al* at the Oxford Orthopaedic Engineering Centre, University of Oxford, and has been implemented in clinical trials at the Nuffield Orthopaedic Centre (Turner-Smith 1990).

The initial clinical trial procedure involved the selection of the femoral and acetabular components and the implantation of reference markers in the bone around the replaced joint.

The bone surrounding the implanted prostheses is marked with 1 mm diameter stainless steel beads. The beads are implanted during the surgical procedure with the aid of an alignment device. Care has to be taken to ensure the beads are placed in positions visible on both x-ray films, but also as far apart as possible to ensure an accurate determination of their position.

The orientation of the equipment used for the x-ray procedure is illustrated in fig. 4.1. The two x-ray tubes are in a convergent configuration with a beam angle of 60° between them. The films are placed perpendicular to the beams to reduce the possibility of image blur and to incorporate the use of "static" or "Bucky" grids. Scatter from dual exposure is reduced by the incorporation of lead frames, fitted with aluminium filters, into the tubes of the calibration frame surrounding the patient.

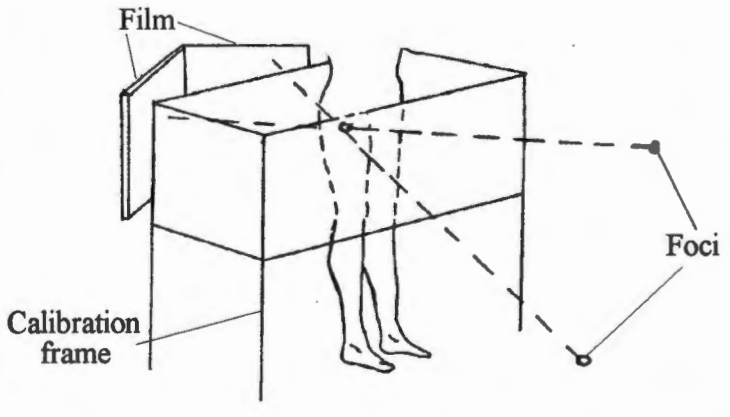

Figure 4.1. The geometry of the equipment assembly used by Turner-Smith (1990).

The patients are x-rayed in a standing position to allow x-ray exposures of both the loaded and the unloaded joint. The standing position also allows the x-ray tubes to be positioned as far as 3 metres away from the patient which increases the clarity of the image on the film, but this configuration places a heavier demand on the x-ray equipment.

An electronic control system is used to expose the two x-rays simultaneously. This reduces the possibilities of errors occurring due to patient movement between exposures. The reported, typical exposure time in this system is 0.8 seconds.

A calibration frame is used to establish the co-ordinates of the system. The calibration frame is manufactured from a light-weight, bonded, epoxy honeycomb material. Attached to the front of the frame is a circuit board with a grid of accurately milled lines which have been filled with bronze putty. The rear of the frame has a similar board attached, which has been covered with a 0.1 mm layer of copper and an identical grid of lines has been created. The precision of the machined grids is reported better than 10 μm (Turner-Smith 1990). The grid line intersections form a co-ordinate system in which the spatial positions of the points may be determined with great precision.

The measurement of the x-rays involves the digitising of the approximately 350 points which include the front and rear grid intersection points, the implanted metal beads and the reference points on the prosthesis. A transparent, electromagnetic digitiser with a resolution of 25 μm is used. The introduction of a CCD image sensing device allows a more precise determination of the centre or edges of points, as well as reducing the visual strains associated with intense measuring. The digitising process is controlled by computer software. This enables an accuracy check to be run to ensure the data entered is accurate with respect to the data to be associated with. The time required for this operation was approximately 45 minutes, but was expected to be reduced as the software was refined.

The analysis of the data involves the use of stereophotogrammetric principles to determine the spatial positions of the reference points on the prosthesis and of the marker beads in the bone.

The ten (or eleven) parameters required to describe the calibration of the central projective geometry were obtained from the three parameters defining the perspective centre (x-ray tube position), the three parameters defining the position of the film, the three parameters defining the orientation of the film and one (or two) parameters defining the scale factors (or each axis of) the measurement system (Turner-Smith 1990).

Projective transformation formulae are used to transform the co-ordinates of the points measured on the x-ray films into the co-ordinates of the one grid system of the calibration frame. Four points each with two co-ordinates are required to perform a transformation. The perspective centres, or the position of the x-ray tubes are determined using the co-ordinates developed through the projective transformations.

The 3-D co-ordinates of the implanted metal beads and the reference points are determined by calculating the mid-point of two theoretically intersecting lines from the x-ray tubes and the co-ordinates determined by the transformations.

The reliability of the measurements indicated a mean value of 0.12 mm with a standard deviation in the co-ordination of the beads of 0.3 mm. This accuracy, indicates the ability to measure the position of beads in the bone in three dimensions to better than 0.2 mm. This is considered sufficient for measuring micromotion in total hip arthroplasty (THA).

4.2. THE LUND SYSTEM

The Lund RSA system was developed by Selvik at the University of Lund in Sweden and submitted as a thesis in 1979 and has been updated and refined for specific applications. Most of this work has been carried out in Lund and in Stockholm.

The clinical procedure for the Lund system involves the implantation of metal beads into the bone surrounding the prosthesis and the introduction of markers into the acetabular component.

Five to eight tantalum beads with a diameter of 0.8 mm are implanted in the bone surrounding the prosthesis during the surgical procedure. The beads are positioned through a cannula and secured in position with bone wax (Kärrholm 1989). For the analysis to succeed at least three beads are required. Implanting the extra beads ensures that sufficient beads will be visible on the x-rays for the analysis.

The femoral components used require no preparation prior to the operation as regular features on the prosthesis are used as reference points. During the analysis phase the centre of the head of the prosthesis is computed and used as one reference point and the lowest point of the tip is computed and used as a second reference point. The acetabular components are made from high density poly-ethylene and require tantalum beads to be added as reference points. The beads are placed in pre drilled holes in the HDPE.

The patients are x-rayed in the supine position, which allows the measurement of the unloaded joint only. The x-ray procedure involves the use of two x-ray tubes positioned above the patient in a convergent, uniplanar orientation. The foci are positioned approximately 0.4 to 0.6 m apart and at a distance of 1 m from the patient. The angle between the foci of the two tubes is approximately 40^{o}. The two x-ray films are exposed simultaneously to ensure no movement of the patient occurs.

A Plexiglas "cage" with embedded tantalum balls, used for the calibration of the system, is shown in fig. 4.2 (Selvik *et al*, 1983). Two of the four walls have 0.5 mm tantalum bead markers cemented to the inside of the two glass plates. The markers closest to the film represent the fiducial marks and are used as the basic co-ordinate system. The markers closest to the foci are the control marks and are used to determine the position of the foci. Photogrammetric instruments are used to determine the 2-D co-ordinates of the fiducial marks and the control points after the construction is completed. The fiducial marks form a co-ordinate system into which all the measured film co-ordinates are transformed.

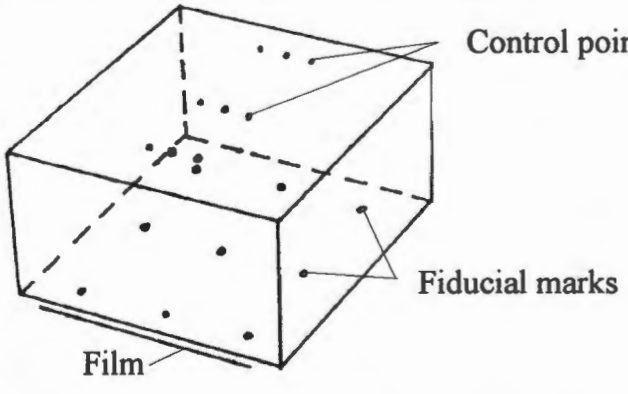

Figure 4.2. A schematic representation of the Plexiglas frame used by Selvik *et al.* (1983)

An advance on the system of a calibration "cage" is a calibration "plate" consisting of a slab of polyurethane foam covered by a polyester shell. A grid system of 6 x 10 holes is drilled through the plate and filled with Plexiglas rods. The rods each have a 1.0 mm tantalum bead at each end. This forms a rectangular lattice which can be placed underneath the patient (Djerf K *et al*, 1987). The construction of this plate conforms to accurate measurements and the positions of the fiducial marks and the control points respective to each other are known. An illustration of the control plate is given in fig. 4.3.

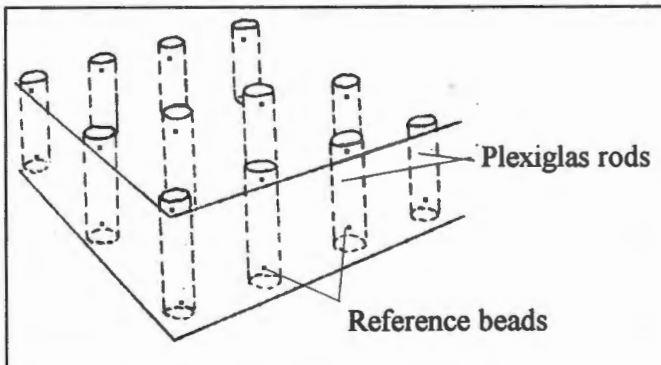

Figure 4.3. A schematic representation of the control plate used by Djerf *et al.*(1987)

The images of the cage and patient markers are identified according to a standard pattern and their 2-D positions measured on a cartographers table or by using a conventional digitizer, with a precision of 5-25 μm. A television camera is used to enlarge the points and make the measuring easier. The 2-D co-ordinate values are stored on a computer.

Five computer programs are used to analyse the measured points for orthopaedic application. The first program XRAY determines the 3-D positions of all the markers. The control markers and the fiducial markers are transformed into the basic laboratory co-ordinate system using projective transformations. KINERR detects and corrects errors in the identification of the markers. KINLAB evaluates the 3-D motions of a rigid body or point and GROWTH records the changes in length between two points. ROTATE re-orientates the object by adjusting the axis direction.

The accuracy of this system has been determined as between 10 and 250 μm (Selvik *et al.* 1983). This is dependant on the quality of the calibration equipment, the image quality, the precision of the measuring equipment and the flatness of the film.

Applications of this system include the assessment of loosening in cemented THR by Mjöberg (1986) and a wear and instability study by Baldursson *et al* (1979). In 1986 Ryd used this technique in a biplanar configuration (with an angle of 90^{o} between the x-ray tubes) to assess the stability of the replaced knee joint. A recent study by Ryd using this RSA method involved the assessment of early fixation in both cemented and non-cemented tibial components (Ryd 1993).

4.3. THE CLEVELAND SYSTEM

The Cleveland RSA system used by Green *et al* (1983) to describe migration of prostheses in total knee and total hip arthroplasties is based on the system described by Brown *et al* (1976) for applications in spinal assessment. The development of the systems took place at Case Western Reserve University, in Cleveland, Ohio, United States of America. Green *et al.* ran clinical trials through the Veterans Administration Hospital and the Department of Orthopaedic Engineering affiliated to the University.

The joint arthroplasty system uses cobalt-chrome beads of different sizes positioned around the implant as internal markers. Three 1.6 mm beads are placed in the cortical bone around the prosthesis and up to six 2.39 mm beads are placed in the cement mantle of the prosthesis (Green *et al.* 1983). The beads in the cortical bone act as reference points in the measurements and are thus assumed to be permanently fixed. This arrangement does not allow measurements of the micromotions at the prosthesis/cement interface but only of movements of the implant/cement composite at the cement-bone interface. Reference points on the actual prosthesis are not required in the system.

A biplanar arrangement is used for the orientation of the two x-ray tubes. A standard and a portable x-ray tube are positioned at 90° to each other in front of a rectangular calibration frame (fig. 4.4).

The calibration frame consists of a set of precisely aligned orthogonal wires in front of, and parallel to each film, and with a marked plexiglass plate parallel to the film. The plate is marked with four lead balls embedded into the plexiglass. The wires form the reference markers for determining the co-ordinates of the film and the lead markers are used to determine the spatial position of the perspective centres of the x-ray tubes. The spatial positions of the cross-wires and the lead balls in relation to each other are known. The patient is positioned between the calibration wires and the plexiglass plate and the x-rays are exposed with the affected joint in non-weight bearing and in weight bearing positions.

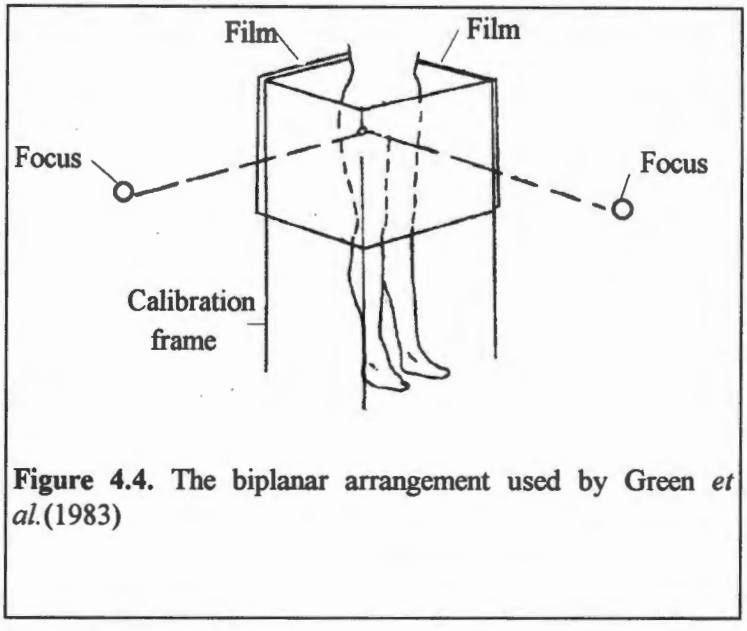

Figure 4.4. The biplanar arrangement used by Green *et al.*(1983)

All the co-ordinates of the reference points are determined using an electromagnetic digitizer with a resolution of 25 μm. The positions of the markers are co-ordinated with reference to the calibration system and thus the positions of all the cobalt-chrome beads can be computed in relation to each other. The resolution of the system is 0.19 mm (Green *et al.* 1983).

The system has been implemented by Green *et al* (1983) to determine the migration and the clinical loosening of total hip and total knee replacements.

4.4. THE SEATTLE SYSTEM

The Seattle RSA system was developed by Veress *et al* at the University of Washington in Seattle, USA. The Departments of Civil Engineering and Orthopaedics as well as the Veterans Administration Medical Centre affiliated to the University were involved in the development of the system (Veress *et al.* 1977). The system was first applied to the tracking of the human patella, but other applications included the assessment of the motion of other skeletal affects such as the subsidence of femoral components in total hip arthroplasty.

The clinical procedure involves the implantation of 0.8 mm tantalum beads in the bone surrounding the affected joint. As with the other RSA systems discussed, the beads are implanted during surgery and establish the internal markers. The implanted components used are standard components and do not have special features added.

The patients are x-rayed standing up-right surrounded by a reference frame. The system uses a convergent x-ray beam orientation with the x-ray tubes positioned approximately 40^{o} to each other. A single film plane is used with the films being attached to the reference frame. The reference frame consists of a *reseau* plate directly in front of the film cassettes and a calibration frame parallel to the *reseau* plate.

The *reseau* plate forms the reference system for detecting problems involving the films, such as film curvature and film movement and comprises a plate with a system of forty five engraved crosses filled with a radiopaque substance form the *reseau* system. A calibration plate used for the determination of the orientation of the x-ray tubes also has forty five engraved markers. All the crosses and markers are co-ordinated after the construction of the frame is complete thus precise positioning of the markers during the construction is not required.

The x-ray phase of the procedure has two parts. Firstly, the frame with the *reseau* plate and calibration plate in place are exposed in order to determine the spatial co-ordinates of the x-ray tubes. For the second part the calibration plate is removed and the patient is x-

rayed in front of the *reseau* plate. The x-rays are exposed simultaneously to ensure no movement of the patient occurs between the successive exposures.

The measurement of the x-ray films involves the digitising of all the points on the x-rays using a co-orddinatograph digitising instrument, with an accuracy of 10 μm, connected to a computer (Lippert *et al.* 1982).

The accuracy of the point determination of the system satisfies the requirement for orthopaedic application of 0.2 mm (Lippert *et al.* 1982*).*

4.5. THE SAN FRANCISCO SYSTEM.

The San Francisco RSA system was developed in the Departments of Radiology, Growth Development and Orthopaedic Surgery at the University of California in San Francisco, USA. The system was described by Hunter et al. (1979) and by Chafetz *et al.* (1984, 1985).

The clinical procedure involves implanting three to five vitallium beads 0.8 mm in diameter, into the shaft of the femur surrounding the prosthesis. The beads are positioned as far apart as possible in order make the determination of the spatial co-ordinates as accurate as possible. Specific positions on standard femoral components are used as reference points. These reference points are the centre of the head of the femoral component and the tip of the stem, which are computed during the analysis stage..

The x-ray procedure uses a single x-ray tube which is moved vertically in order to obtain the two x-ray exposures. The x-ray tube is positioned approximately 1.80 m away from the film and is shifted by approximately 15° (Hunter *et al.* 1979). These values are calculated precisely through later computation.

A fixed calibration frame, attached to the film cassette, surrounds the patient during the exposures. The frame has four fixed radiopaque markers in the front and rear planes whose spatial orientation with respect to one another is accurately known. The patient is

required to remain as still as possible, while the tube is shifted from one position to the next during the procedure, to limit the errors which will result in the determination of the 3-D co-ordinates of the internal markers.

The x-ray exposures are analysed using an ultrasonic digitizer and a minicomputer (Hunter *et al.* 1979). The marker points surrounding the patient externally as well as those surrounding the prosthesis internally are located and digitised. From the 2-D co-ordinates the 3-D co-ordinates are calculated and a 3-D co-ordinate map is generated for each stereo pair of x-rays. The origin of the co-ordinate system is the centre of the head of the prosthesis. The line between the origin and the tip of the prosthesis forms the x-axis of the co-ordinate system. The mid-point of this line forms the component reference point. The XY plane is a plane perpendicular to the x-axis through an implanted bead. The subsidence of a femoral component is measured as a change in the distance between the component reference point and a line from the centre of a group of beads projected onto the x-axis as is illustrated in fig. 4.5.

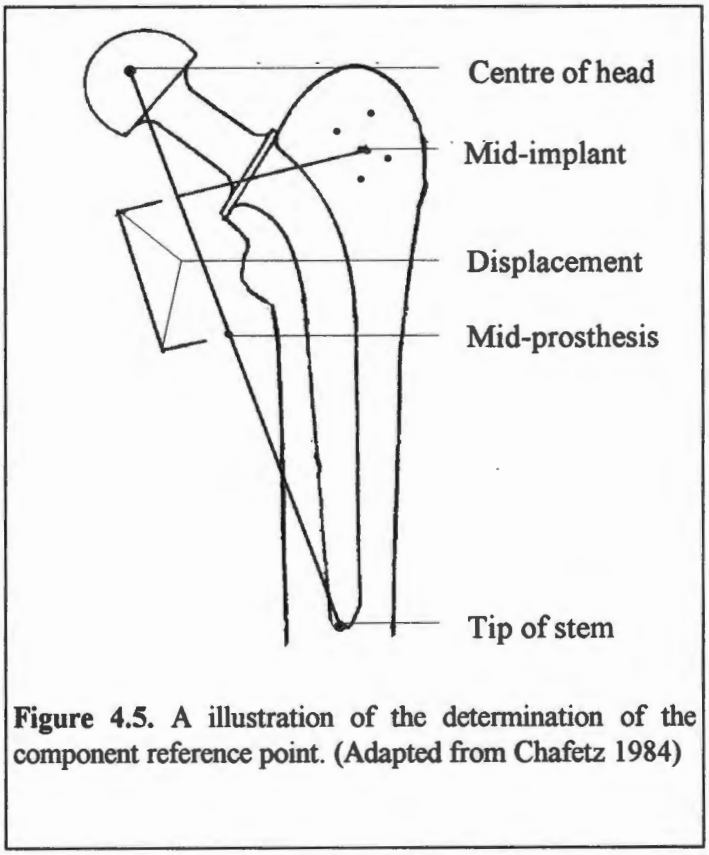

Figure 4.5. A illustration of the determination of the component reference point. (Adapted from Chafetz 1984)

The accuracy of the system applied to studies using dry bones implanted with prostheses, indicate a reproducibility accuracy of 0.3-0.5 mm (Hunter *et al.* 1979), but much larger errors, in the order of 0.6 mm are encounted in measurements involving patients (Chafetz et al. 1985) These errors are attributed to the patient movements between the successive x-ray exposures.

CHAPTER 5
MATERIALS AND METHODS

The system of x-ray stereophotogrammetric measurement used in this study involves the use of two video cameras and a single, stationary x-ray source to obtain all the necessary information to detect and measure subsidence of the femoral component in total hip arthroplasties. The use of video cameras makes it possible to correct for slight movements of the patient or the control frame during successive x-ray exposures. This solves the problem of requiring two x-ray tubes to take simultaneous exposures. The software for the digitising and calculation of the three-dimensional co-ordinates of the internal markers was developed from existing software in the Biostereometrics group of the Department of Biomedical Engineering. The system was initially tested and refined using dry bones implanted with prostheses and beads. All the equipment designed for the system was, however, designed with a patient of average build in mind.

5.1 EQUIPMENT FOR DATA CAPTURE AND COMPUTERISED ANALYSIS

The equipment used in the study may be grouped into the following categories: i) **image capture equipment** including the x-ray tube, two CCD cameras fitted with zoom lenses for the bone specimen studies and fixed focus lenses for the patient studies, a lamp, a video monitor and an image mixer; ii) **computer and measuring equipment** consisting of a personal computer and monitor with an image processing card and a digitising tablet; iii) **calibration and patient related equipment**: a control frame with 3-D co-ordinated control points on a stand, a turn-table, dry bones, prosthetic femoral components, 0.8 mm Tantalum beads, background blackening sheets, low stool and a holding clamp, a black

cover garment for the patient, perspex marker holders and velcro strips; and iv) 2.3 mm stainless steel ball bearings and a reflex microscope for **accuracy testing**.

5.2 MATERIAL PREPARATION

5.2.1 CONTROL FRAME

The control frame is a metal structure, supported on a metal stand, designed to serve as a calibration device, a patient support and a x-ray cassette holder (fig. 5.1). The construction of the frame need not prescribe to accurate measurements as the precise locations of the necessary calibration points are determined after the construction is complete.

Figure 5.1. The control frame and stand

The frame and the stand are constructed from steel square tubing. The frame is 850 mm in length, 440 mm in height and 480 mm in depth. The front and back panels of the frame have a 9 x 4 grid system made from tightly stretched piano wire. A backing frame with a wooden board has been added 50 mm behind the rear grid to form a support for the x-ray cassette. The front and rear panels are joined by two pieces of tubing on the right side. The left side of the frame has been left open to allow easy access by the patient. The vertical frame members at each corner fit over the vertical stand members and are secured at the desired height by four screw-clamps. The vertical members of the stand are 1000 mm high which allows for sufficient height variations to accommodate patients of different heights.

The three-dimensional co-ordinates of the grid intersections have been determined by a land surveyor using conventional surveying techniques. The 72 grid intersections are numbered in order to simplify the task of identifying the intersection required. Four 1.2 mm metal ball bearings have been positioned on a horizontal wire to aid in the identification of the front panel intersections on the x-ray films and two metal ball bearings on a vertical wire identify the rear intersections.

5.2.2 TURN-TABLE

X-ray stereophotogrammetry requires two x-ray exposures to be taken from different perspectives. In order to reduce the patient stress and fatigue involved in the x-ray tube being moved and re-aligned a turn-table has been incorporated into the system to allow the patient to be rotated in front of the stationery x-ray tube.

The circular turn-table is a wooden structure which fits over the base of the control frame stand (fig.5.2). The two circular wooden plates are 450 mm in diameter and 20 mm thick. The base plate has four metal rollers positioned around a central hole. The upper plate has a metal rod attached to the centre which fits into the central hole in the base plate. Five

stopper blocks have been placed around the edge of the base plate to provide extra stability in the event of a patient leaning too heavily on the edge of the turn-table. The underside of the turn-table has four rubber stoppers which raise the structure to fit over the base frame of the stand. This arrangement has the added advantage of the mass of the patient on the turn-table providing additional stability to the control frame set-up.

Figure 5.2. The turn-table

The primary function of the turn-table is to provide a mechanism for rotating the patient between successive x-rays. To facilitate this a series of seven holes has been drilled into the front edge of the lower plate, at 10° intervals. A braking key fits through a hole in the upper and one of the holes in the lower plate, and thus prevents the upper plate from spinning around on the rollers.

5.2.3 CAMERA STAND

The camera stand has been designed to be positioned beneath the x-ray tube and to have the capability of adjusting the camera base and the camera height (fig.5.3).

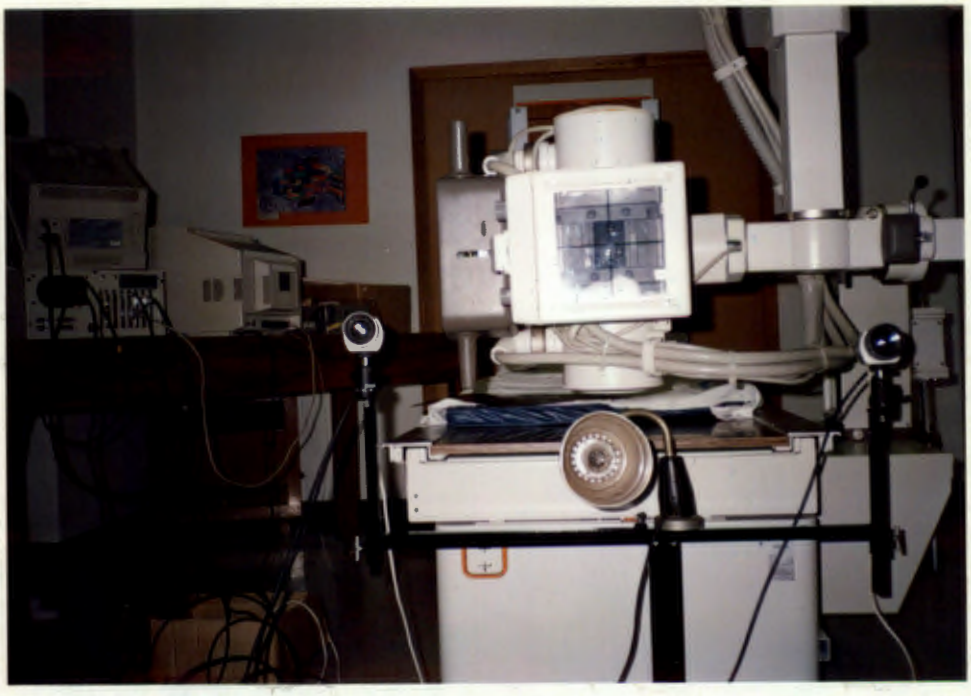

Figure 5.3. The camera stand

The stand consists of an adjustable horizontal bar to allow the camera base to be changed, with adjustable vertical bars fitted at each end to adjust the camera height. Two plates are attached to the tops of the vertical bars to accommodate the cameras.

The camera stand allows the cameras to be positioned at heights between 550 mm and 860 mm and with a camera base between 520 mm and 1000 mm.

5.2.4 SUBJECT PREPARATION

Dry bones were used to simulate the situation in patients for the preliminary tests. In order to obtain conclusive results from the method it is necessary to introduce reference markers into the measuring area. For the camera/x-ray system two sets of reference markers are required. A set of internal markers consisting of metal beads implanted during surgery and a set of external markers added externally at the time of the x-ray .

An orthopaedic surgeon implanted retrieved femoral components into three dry bones and placed metal beads into the bone around the prostheses. In the first specimen the implanted beads were commercial steel ball bearings with a diameter of 1.2 mm. After measuring the first test specimen all subsequent test specimen bones were implanted with 0.8 mm tantalum beads. Five or six beads were positioned in each bone as close to the actual position that the beads would occupy in patients as possible. A minimum of three beads, suitably disposed, is required in order to run the calculation program and therefore implanting additional beads ensures the minimum number of beads are always visible and thereby introducing redundancies which allow for least square comparison solutions. In general two beads are placed in the region of the greater trochanter, two in the region of the lesser trochanter and one each in the medial and lateral aspects of the femoral shaft in the area of the tip of the prosthesis. A detailed description of the bead placements is given in Appendix C. The bone/prosthesis/bead combination will hence forth be referred to as the bone specimen.

Four external markers were attached to the bone specimen at the time of x-raying. The external markers consist of crosses of thin wire, for identification on the x-ray images, attached behind 5 mm discs of retro-reflective material, for identification on the video images. The discs are stuck onto two strips of thick card painted matte black and are attached to the bone specimen as shown in fig.5.4.

Figure 5.4. One of the dry bone specimens showing the implanted femoral component and the positions of the external markers

On one bone specimen five 2.3 mm steel beads were glued onto the greater trochanter for measurement under the reflex microscope, as a test of the accuracy of the x-ray digitising process (fig.5.5).

The patients were initially prepared for the procedure during surgery: the surgeon implanted five to six 0.8 mm tantalum beads into the bone surrounding the implanted joint in the positions described in Appendix C.

Figure 5.5. The bone specimen with the accuracy beads glued in position.

External markers are positioned around the patient at the time of the x-ray procedure. A black garment has been made in order to cover the clothing of the patient and to ensure adequate contrast with the markers. Two strips of thick velcro were secured around the upper thigh of the implanted leg over the black garment. The external markers are similar to those used in the bone specimens and consist of two strips of black perspex, with velcro backing. The strips are attached to the velcro strips on the patient (fig.5.6) in such a way that the four external markers are placed closed to the measuring area and so that the markers and the femur move as a rigid body .

Figure 5.6. The black cover garment and external markers used for the patient studies.

5.2.5 CAMERAS, MIXING, LIGHTING AND MARKERS

Two Burle TC625EX CCD (charge coupled device), solid state matrix cameras fitted with zoom lenses with a focal distance of 12,5 - 75mm and an aperture "f stop" of 1,8 are used for the bone specimen studies.

The analogue images from the cameras are converted to digital quantities by means of image processing card in the computer and the images are displayed an a CCTV (closed circuit TV) monitor. A PIP MATROX analogue to digital (A-D) converter image processing card was used.

The images from both cameras are displayed simultaneously on the monitor through the use of an image mixer. The image mixer has two different types of settings which allows the user to determine the mix required. The settings control the vertical and horizontal mixes and the screen can therefore be adjusted to obtain the best possible mix for the particular circumstance. For this study the screen is "split" vertically down the centre (fig.5.7). The image mixer used for this study is a Primebridge Micro-series image mixer (Model RVW-1).

Figure 5.7. The "split" screen images on the video monitor.

The lighting is crucial to the accuracy of the system. The images from the cameras are digitised from the monitor and therefore the control points and external markers are required to be as clear and as well defined as possible. As mentioned previously, the grid intersections on the control frame are marked with retro-reflective discs as are the external markers. A direct light source on the retro-reflective markers ensure the best possible image on the monitor. All the surfaces which could affect the direct light source are either

painted matte black or covered with black sheets. This prevents any reflected light interfering with the markers. The interference of the reflected light causes the markers to be registered as different sizes on the monitor which in turn causes problems with accuracy in the digitising process. The size and brightness of the markers on the monitor is adjusted by adjusting the camera settings.

The markers for this study are retro-reflective discs 5mm in diameter for the camera images and metal targets for the x-ray images. The most important consideration in the positioning of the external markers is the distance between the respective markers. The further apart these markers are within the measuring area the better. The digitised values of the marker co-ordinates outside the measuring area may be extrapolated but this affects the overall accuracy of the system.

5.3 EQUIPMENT SET-UP AND DATA CAPTURE AT PRINCESS ALICE ORTHOPAEDIC HOSPITAL (PAOH)

For the bone specimen studies, the x-ray tube is positioned approximately 2 m away from a side wall of the x-ray room and at a height of approximately 1m from the floor. All the other equipment is positioned around the x-ray tube. In the patient studies the x-ray tube was positioned 1.15 m away from a permanent "Bucky" stand. The stand was equipped with a sliding mechanism for rapidly changing the x-ray cassettes.

The wall facing the x-ray tube, or the "Bucky" stand, was covered with a black sheet and the control frame positioned directly in front of the x-ray tube. The turn-table is placed over the base of the stand with the graduated holes and braking key facing the front. The height of the frame adjusted such that the centre of the front panel is in line with the x-ray tube positioned to approximately average hip height.

The camera stand is positioned beneath the x-ray tube and the vertical and horizontal adjustment bars are adjusted so that the cameras are equidistant from, and in line with the centre of the x-ray tube. The "base-height" ratio of the cameras with respect to the target distance is adjusted to ensure this ratio is approximately 1:3. The cameras are attached to the stand by means of ball and socket connectors to allow for the fine adjusting of the position of the images on the monitor. A single light source is clamped onto the camera stand between the two cameras. The system is schematically represented in Appendix E.

The cameras are connected to the image mixer which in turn is connected to the image processing card in the computer and the monitor.

From this point hence the procedure is run by a menu driven computer package written for this study. The first part of the procedure is the calibration of the cameras. Using the menu driven commands, the camera images are called up onto the monitor. The cameras and image mixer are manipulated until the images on the monitor are acceptable. An acceptable image has the required number of control points visible, and the left and right images the same size and orientation on the screen.

The image of the control frame is captured by the computer and stored on a disc. Once the control image has been captured the cameras may not be moved (Ruther and Adams, 1984). If the cameras do move the calibration procedure has to begin again. This procedure is followed each time the cameras are moved or if a gross movement of the control frame takes place. The calibrated system may be used to x-ray and film a number of consecutive bone specimens and patients before re calibration becomes necessary.

The data-capture involves a x-ray film being exposed and a camera image being captured simultaneously. For the bone studies an x-ray film cassette was placed in the cassette holder behind the control frame and the bone specimen introduced into the control frame. The bone specimen was held in a vice-clamp and placed on a low stool positioned on the

turn-table, with the greater trochanter and the head of the prosthesis in the centre of the marked reference field. The film was placed in the "Bucky" frame for the patient exposure.

The first x-ray film was exposed and the camera images captured simultaneously by the radiographer. The x-ray film cassette was replaced while the specimen or patient was rotated on the turn-table. The second x-ray and camera images were captured simultaneously. The first x-ray exposure is termed the left x-ray exposure and the second x-ray exposure is termed the right x-ray exposure. A summary of the data capture is illustrated in figure 5.8.

The set-up may immediately be readied for another specimen or patient. All the captured data was stored on a computer disc with a individually discreet file name per patient. To avoid any possible identification problems each patient's data was stored on a separate disc.

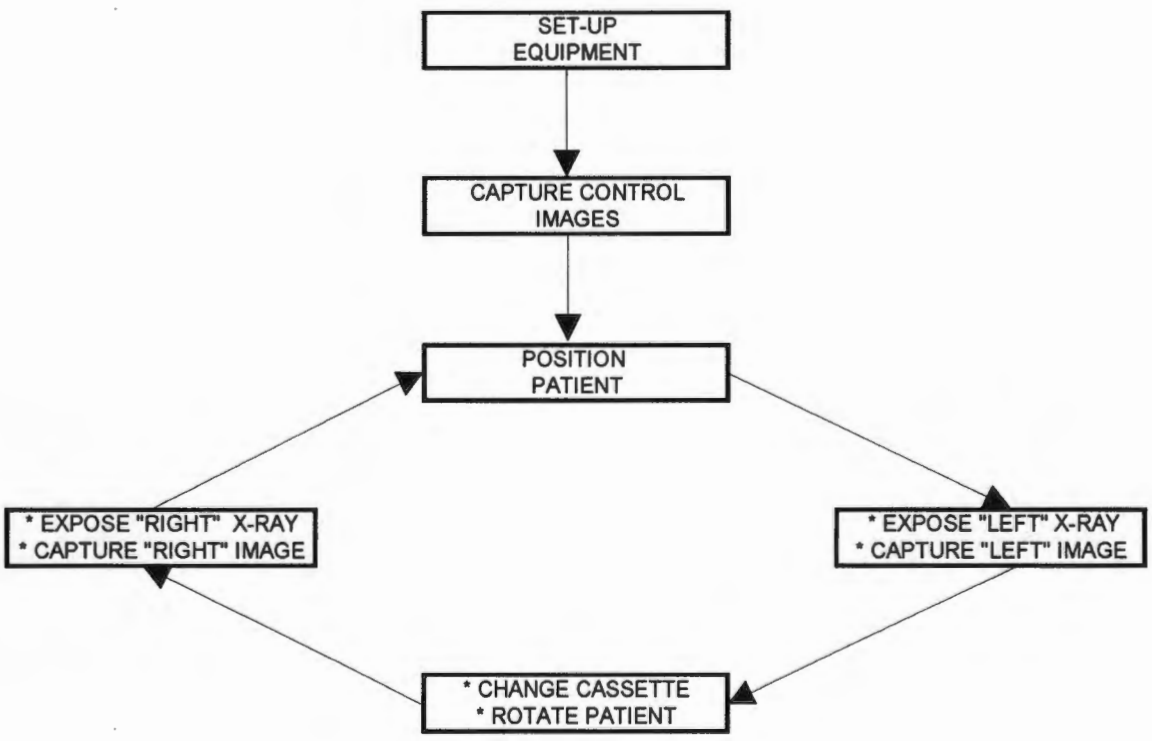

Figure 5.8 Summary of the Data Capture phase.

5.4 DATA ANALYSIS AND CALCULATIONS

5.4.1 DIGITISING OF VIDEO IMAGES

All the video images are digitised using the computer key board and the video monitor. The program re configures the keyboard number pad to allow the user to move the cursor around the monitor screen rapidly. This allows for horizontal and vertical movements of 25 pixels as well as single pixel movements in the same directions. For the duration of the digitising process the computer screen displays a representation of the possible movements and the appropriate computer keys (fig.5.9).

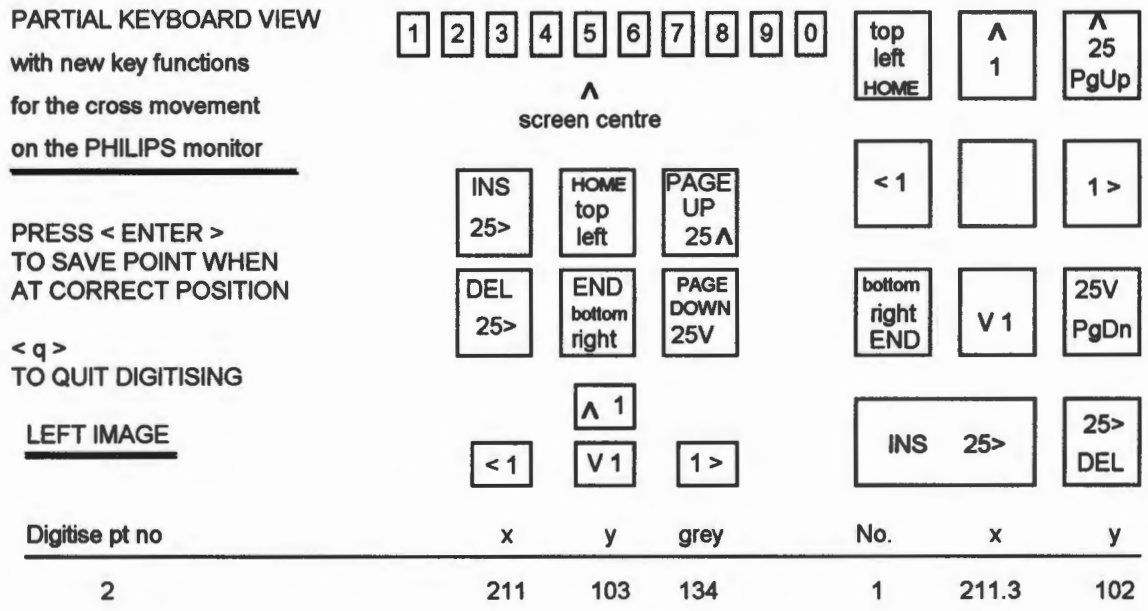

Figure 5.9. The computer screen display of the instructions for the video digitising process.

Using the appropriate keys, the cursor is moved across the screen until the centre of the cursor is approximately in the centre of the "white dot" formed by the retro-reflective target. The user selects this approximate centre and the computer determines the mathematical centre by finding the centre of gravity of the grey values surrounding the point. It is primarily for this reason that the area surrounding the markers should be as dark and as non-reflective as possible.

The digitised information is automatically stored under the patients file name with a descriptive suffix. The computer assigns specific descriptive suffixes to the original file name, depending on the procedure being followed. The set of co-ordinates for each video image that is digitised will have the same file name with a different suffix.

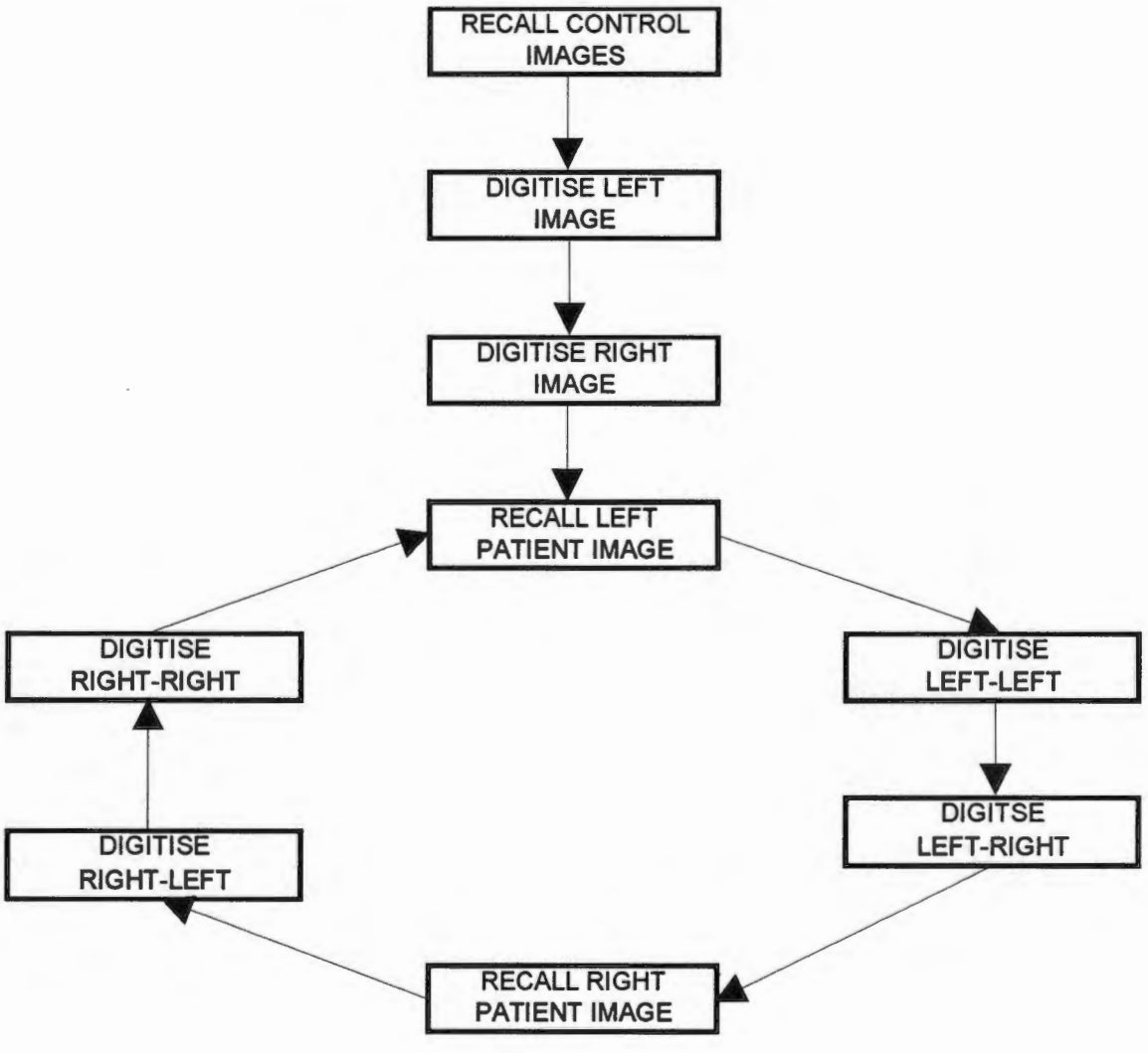

Figure 5.10 Summary of the Video Digitising process

The digitising of the video images is divided into two sections viz. the digitising of the "empty" control images and the digitising of the patient images. Each captured image is comprised of an image recorded by each of the cameras. These images are named according to the position of the camera which recorded that section of the image. Thus

each recorded image consists of a left and a right image portion which have to be digitised separately. The control has two images to be digitised, a left image and a right image and each specimen or patient has four images to be digitised viz. a left and right image for each of the two positions recorded.

In the case of the control images the cameras are set in such a way so as to guarantee that all the marked control points appear on both the video images. This is to ensure that as many control points as possible are used to determine the parameters of the cameras in order to keep the accuracy as high as possible.

The control points are numbered and are digitised strictly according to that number sequence.

The patient images are digitised in a similar fashion to the control points. To locate the position of the patient in the control frame four control points are digitised first and then the four external markers are digitised. The presence of a patient in the control frame obscures the majority of the rear control markers. Appendix D shows a print of a patient image. As the control has previously been digitised the position of the rear markers relative to the front markers is known and only the four front corner markers are digitised. A summary is given in figure 5.10.

5.4.2 DIGITISING OF X-RAYS

A set of two stereo x-rays per specimen or patient are digitised to determine the precise location of the internal markers and the prosthesis. The x-rays are digitised individually using a digitising instrument. The computer program requires only the control points and marker points visible on both x-rays to be digitised. All the control frame intersections can be determined from the extrapolated straight lines (fig. 5.11). The order of digitising is again important as the programme reads the files according to the order of input. The

control points are entered in numerical order followed by the external body markers and finally the internal bead points are entered.

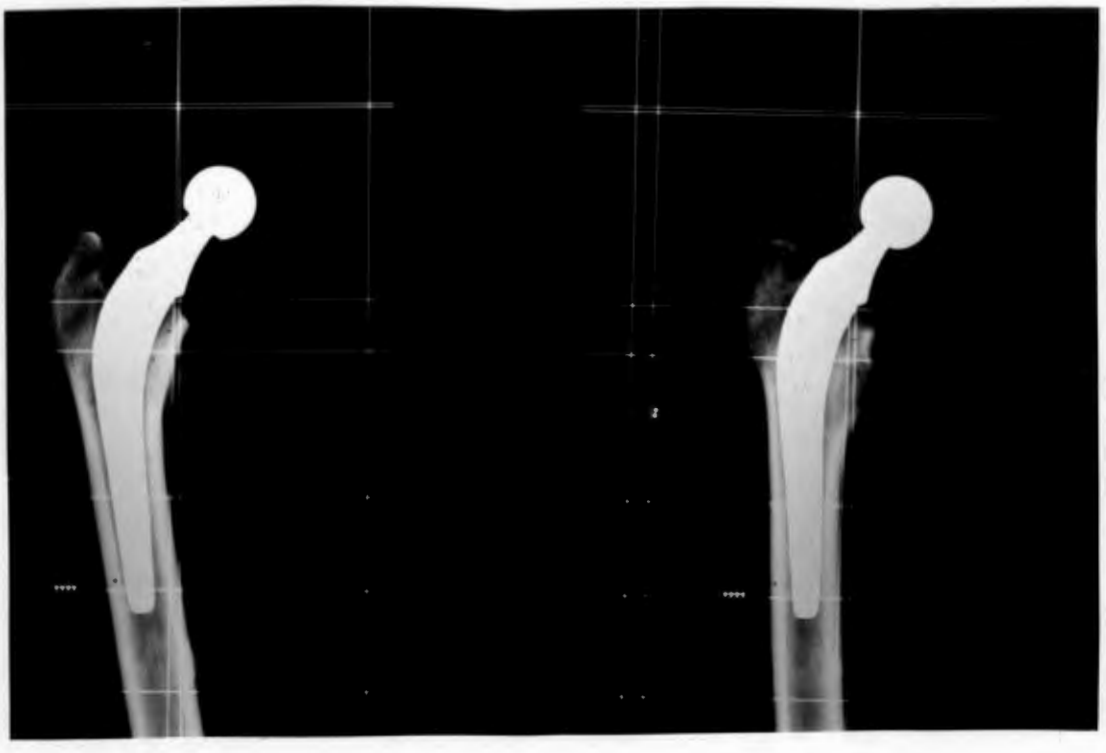

Figure 5.11. An example of a stereo pair of x-rays showing the control frame grid lines.

In order to determine the subsidence of the prosthesis reference points on the prosthesis are required. The three-dimensional co-ordinates of these reference points are compared to the three-dimensional co-ordinates of each of the internal bead points. From these comparisons it becomes possible to determine the nature of any movement which may have occurred.

The head of the prosthesis is assumed to have a spherical shape of which the centre may be mathematically determined with a high degree of accuracy. The centre is used as the first reference point. This is achieved by measuring a number of points around the circumference of the head and, by using a sequence of equations the three-dimensional co-ordinates of the centre of the head is computed. The sequence of equations used for these

calculations is presented in detail in Appendix A following the methodology described by Baldursson *et al.* (1979).

The lowest point on the stem of the prosthesis with a hemispherical tip is used as a second reference point. This point is calculated by fitting a second order polynomial equation to points digitised along the length of the prosthesis and around the tip and mathematically determining the turning point of the curve. Problems with the mathematical determination of the turning point are encounted, however, when a flat tipped prosthesis is used.

In order to determine the three-dimensional co-ordinates of the internal bead points and the reference points on the prosthesis with greater accuracy the program is designed to allow these points to be measured three times each and a mean value calculated. The mean is then used to calculate the three-dimensional value.

5.5 DETAILED CALCULATION OF THREE-DIMENSIONAL CO-ORDINATES

The calculation of the three dimensional co-ordinates of the internal bead markers and the reference points on the prosthesis involves a series of calculations which determine the mathematical rotations and transformations. The equations used are described in detail in Appendix B. The software written for the project, using the theory of projective transformations, has been designed to accommodate any accidental movement of the control frame and also any movements of the patient. The control frame markers act as reference points for any frame movement and the external body markers are used to determine any patient movement. The calculations may be divided into two sections: firstly, the calculations using digitised 2-D co-ordinates from the video images and secondly, the calculations using the co-ordinates digitised from the x-ray exposures.

5.5.1 VIDEO IMAGE CALCULATIONS

The first calculation is to determine the transformation parameters (b-parameters, or camera constants) for the cameras from the co-ordinates digitised from the "empty" control frame, using projective transformations. These parameters relate the spatial position of the cameras to the position of the control frame and the contents thereof. The b-parameters are then used to determine the three-dimensional co-ordinates of the four front control points and the four external markers digitised from the two sets of video images.

In order to account for any accidental movement of the control frame as the patient enters the frame, the three-dimensional co-ordinate values of the four front control points of the left set of video images are used to determine the three dimensional transformed co-ordinate values for the whole control using Caley's formula and the Rodriques parameters (Thompson, 1969). The transformed values become the "new" three-dimensional co-ordinate values of the control grid intersections. This "new" control is termed a **LH ROTATED CONTROL** and forms the control system used to determine the b-parameters for the left x-ray exposure. The same procedure is performed on the four front control points and the external markers on the right set of video images. The "new" control for the right set of video images is termed a **RH (FIRST) ROTATED CONTROL**.

Further transformations are required to create the control system to determine the parameters for the right x-ray exposure. The calculated three-dimensional co-ordinate values of the external markers in the RH (FIRST) ROTATED control are transformed (rotated and translated) into the LH ROTATED system. The transformation parameters derived from this transformation are used to transform the RH (FIRST) ROTATED control into the RH (DOUBLY) ROTATED control system. This is the control system used to determine the b-parameters for the right x-ray exposure.

5.5.2 X-RAY EXPOSURE CALCULATIONS

In theory an x-ray image or picture may be assumed to be a central projection and thus the x-ray focus may be assumed to be a perspective centre as is the case of a normal camera lens. Therefore the b-parameters for the left and right x-ray exposures may be calculated using the geometry of projective transformations (Appendix A) in which the control system co-ordinates are derived through the video image calculations. The LH ROTATED control system co-ordinates and the digitised values from the left x-ray exposure are used to calculate the b-parameters for the left x-ray exposure. The RH (DOUBLY) ROTATED control system and the right x-ray exposure are used to calculate the right exposure b-parameters.

The three-dimensional co-ordinates of the external and internal markers as well as the co-ordinates of the reference points on the prosthesis are calculated from the digitised values using the calculated b-parameters.

5.5.3 CALCULATION OF THE DISTANCES

The distances between all the bead points and the two reference points on the prosthesis are calculated. The calculations are based on the co-ordinate values determined by transforming the control systems of the successive x-rays into a common system and then calculating the co-ordinate values of the internal bead points as if all the x-rays where exposed in exactly the same position. Following the calculation of the co-ordinate values it is then possible to determine the distances between each bead and the centre of the head of the prosthesis and the tip of the prosthesis. These distances indicate the magnitude of the movement of the prosthesis as well as the approximate direction.

5.6. EXPERIMENTAL PROCEDURE

The evaluation of the system is based on the data acquired from stereo pairs of x-rays and video images of bone specimens and from a group of THA patients. The data capture and analysis phases followed the method described above.

5.6.1 EVALUATION OF THE ACCURACY OF THE SYSTEM

The three co-ordinates *(x,y,z)* of each of the five externally mounted beads were determined by digitising and then by measuring the same beads five times under the reflex microscope. The Reflex microscope (Reflex Measurement Ltd. London, UK) is a precision instrument with an accuracy of 4 μm for the *X* and *Y* co-ordinates and 15 μm for the *Z* co-ordinates as claimed by the manufactures. Reported results for the accuracy of the microscope are ±2 μm for the *X* and *Y* co-ordinates and 4 to 8 μm for the *Z* co-ordinates depending on the depth perception of the observer (Adams and Wilding 1988). The co-ordinates derived from the Reflex microscope measurements were considered to be an error free control. The mean co-ordinate values for the five measurements were transformed into a common system by calculating the Rodriques parameters of the first system (digitised values) and using the parameters to transform the second system (microscope values). The transformation allows the two sets of results to be compared directly and the accuracy to be determined by calculating the difference between the co-ordinates (table 6.1).

The 3-D distances between the five beads were calculated using the following formula:

$$\text{3-D Distance} = \sqrt{(x_1 - x_2)^2 + (y_1 - y_2)^2 + (z_1 - z_2)^2} \ .$$

The difference between the distances was calculated by subtracting the distance determined using the co-ordinates measured by the reflex microscope (distance A) from the distance determined using the digitised values (distance B) (table 6.2).

5.6.2. INTER-OBSERVER COMPARISONS

A complete set of measurements for a stereo pair of x-ray exposures was measured four times each by two different observers. From the calculated co-ordinates the distances between each internal bead and the surrounding beads was calculated using the previously mentioned formula. A mean was taken for each respective distance as measured by the two observers and compared (table 6.3).

5.6.3. REPEATABILITY / INTRA-OBSERVER ACCURACY

The repeatability was assessed by digitising and calculating the co-ordinates of the internal beads on a set of x-ray exposures five times in the first case and three times in the second case for one observer and four times in the case of a second observer. The distances between the beads were determined and a mean was calculated for each distance which was compared using the standard deviation (tables 6.4-6.6).

5.6.4 ACCURACY OF DETERMINING THE CENTRE OF THE HEAD AND THE CO-ORDINATES OF TIP OF THE STEM OF THE PROSTHESIS.

The co-ordinates of the centre of the head of the prosthesis and of the tip of a hemispherical prosthesis were determined five times from the same set of x-rays using the software based on the equations detailed in Appendix A. The mean and standard deviation of the co-ordinates of the two points were determined and compared (table 6.7-6.8).

5.7 A SIMULATED PATIENT FOLLOW-UP

In order to evaluate the performance of the system in a patient follow-up situation the bone-specimens were x-rayed three times. Between each successive stereo x-ray pair the bone-specimen was removed from the control frame and then repositioned. The stereo x-ray pairs were processed as follow-up series with the same file names except for a number

identifying the position in the series. The results were evaluated according to the accuracy in co-ordinating the beads, the calculated distances between the beads and the distance between the head and the tip on three sets (table 6.9-6.11).

In order to evaluate possible subsidence by the femoral component, a bone specimen was x-rayed twice. Between the pairs of exposures the specimen was removed from the control frame and the head of the component tapped lightly to cause the component to "subside". The movement was reported as a variation in the distances between specific beads and the centre of the head and the tip of the stem of the prosthesis (table 6.12-6.14).

5.8 INITIALISATION OF PATIENT TRIALS

The system was implemented in clinical trials and evaluated with regards to the suitability when used with patients and also the ability to measure the rotations of the patient accurately. An example of a patients x-ray is shown in figure 5.12.

The procedure for the bone specimen studies was followed with minimun adjustments required. The x-ray tube was moved closer to the frame in order to be used with the stationery "Bucky" and the camera zoom lenses were replaced by fixed focus lenses.

Figure 5.12. A patient x-ray showing the implanted beads, external markers (crosses) and prosthesis.

CHAPTER 6
EVALUATION

6.1 ACCURACY OF THE X-RAY DIGITISING PROCESS

Table 6.1 refers to the accuracy accomplished in the x-ray digitising process in determining the *x,y,z* co-ordinates of the beads as compared to the co-ordinates determined by the reflex microscope, which was considered to be an error free control system.

BEAD NUMBER	DIFFERENCE Dx (mm)	DIFFERENCE Dy (mm)	DIFFERENCE Dz (mm)
1	0.20	0.07	0.15
2	0.13	0.05	0.04
3	0.21	0.15	0.06
4	0.16	0.09	0.13
5	0.03	0.13	0.08

Table 6.1. The accuracy between the digitised co-ordinates and measured co-ordinates.

The differences range between 0.03 mm and 0.21 mm indicating the digitising process is able to determine the three co-ordinates defining a point to a accuracy of ±0.2 mm..

The 3-D distances between the beads, calculated from the 3-D co-ordinates, are given in table 6.2.

The mean of the differences was calculated as 0.24 mm with a standard deviation of 0.11 mm. This result correlates with the accuracy determined previously, when determining the co-ordinates of a point, of ± 0.2 mm.

BEAD NUMBERS	DISTANCE A (mm)	DISTANCE B (mm)	DIFFERENCE (mm)
1 & 2	10.40	10.17	0.33
1 & 3	16.96	16.48	0.48
1 & 4	18.30	18.13	0.17
1 & 5	27.29	27.17	0.12
2 & 3	12.55	12.33	0.22
2 & 4	21.57	21.35	0.22
2 & 5	23.14	23.27	-0.13
3 & 4	13.89	13.66	0.23
3 & 5	10.99	11.31	-0.32
4 & 5	16.91	16.75	0.16
MEAN OF DIFFERENCES (mm)			0.24
STANDARD DEVIATION OF DIFFERENCES			0.11

Table 6.2. Calculated distances between the beads with distance A representing the distances calculated using the reflex microscope measurements and distance B those calculated using the digitised values.

6.2. INTER-OBSERVER COMPARISONS

Table 6.3 reflects the comparisons of the mean distances between the internal bead points in a bone-specimen as measured by two observers BvG and BG.

BEAD NUMBERS	MEAN DISTANCE: OBSERVER BvG (mm)	MEAN DISTANCE: OBSERVER BG (mm)	DIFFERENCE (mm)
1 & 2	42.18	42.09	0.08
1 & 3	42.03	42.05	-0.02
1 & 4	37.70	37.43	0.27
1 & 5	47.83	47.71	0.12
2 & 3	10.68	10.72	-0.04
2 & 4	25.38	25.16	0.22
2 & 5	45.13	44.75	0.38
3 & 4	18.11	17.89	0.22
3 & 5	36.55	36.26	0.28
4 & 5	20.04	19.85	0.20
MEAN OF DIFFERENCES (mm)			0.14
STANDARD DEVIATION OF DIFFERENCES			0.08

Table 6.3. Differences in distances determined by two observers.

The mean of the differences is 0.14 mm with a standard deviation of 0.08 mm indicating a good correlation between the determinations of different observers.

6.3. REPEATABILITY

The results of the intra-observer evaluations (repeatability) are shown in table 6.4, 6.5 and 6.6.

DIST. No.	MEASUREMENT NUMBER / DISTANCE (mm)					MEAN	STD. DEV'N
	1	2	3	4	5		
1	42.13	42.08	42.22	41.68	41.94	42.05	0.13
2	42.15	41.85	42.26	41.93	41.68	41.97	0.23
3	37.22	37.40	37.62	37.10	37.48	37.36	0.21
4	47.49	47.71	47.72	47.92	47.61	47.69	0.16
5	10.56	10.89	10.57	10.87	10.89	10.76	0.17
6	25.01	25.21	25.11	25.32	25.22	25.17	0.12
7	44.70	44.70	44.70	44.90	44.80	44.76	0.09
8	17.88	17.89	17.91	17.89	17.87	17.89	0.01
9	36.37	36.19	36.23	36.26	36.30	36.27	0.07
10	19.94	19.74	19.85	19.86	19.84	19.85	0.07
MEAN OF STANDARD DEVIATIONS							0.13

Table 6.4. Standard deviation of the repeatability of ten distances measured five times by observer BG.

DIST. NO	MEASUREMENT NUMBER / DISTANCE MEASUREMENT (mm)			MEAN	STD. DEV'N
	1	2	3		
1	10.34	10.20	10.32	10.29	0.18
2	16.59	16.90	16.49	16.66	0.21
3	17.79	18.14	18.03	17.99	0.18
4	27.09	27.25	27.51	27.28	0.21
5	12.29	12.77	12.34	12.47	0.26
6	21.01	21.35	21.28	21.24	0.13
7	23.07	23.32	23.61	23.33	0.27
8	13.49	13.51	13.34	13.45	0.09
9	11.12	11.09	11.68	11.30	0.33
10	16.69	16.65	16.69	16.69	0.02
MEAN OF STANDARD DEVIATIONS					0.18

Table 6.5. Standard deviation of the repeatability of ten distances measured three times by observer BG.

The standard deviations determined from the difference measurements ranged between 0.02 mm and 0.33 mm in the two sets of results. The means of the standard deviations are between 0.13 mm and 0.18 mm. The results indicate a consistency of measurement upto ± 0.3 mm.

DIST. NO	MEASUREMENT NUMBER / DISTANCE MEASUREMENT (mm)				MEAN (mm)	STD. DEV'N
	1	2	3	4		
1	42.25	42.06	42.20	42.19	42.18	0.08
2	42.33	41.87	42.02	41.90	42.03	0.21
3	37.65	37.85	37.83	37.48	37.70	0.17
4	47.94	48.00	47.62	47.75	47.83	0.17
5	10.57	10.80	10.76	10.60	10.68	0.11
6	25.42	25.35	25.45	25.31	25.38	0.06
7	45.02	45.11	45.00	45.40	45.13	0.18
8	18.16	18.25	18.04	17.98	18.11	0.12
9	36.56	36.57	36.23	36.82	36.55	0.24
10	19.86	20.07	19.87	20.37	20.04	0.24
MEAN OF STANDARD DEVIATIONS						0.16

Table 6.6. Standard deviation of the repeatability of ten distances measured four times by observer BvG.

6.4 ACCURACY OF DETERMINING THE CENTRE OF THE HEAD AND THE CO-ORDINATES OF TIP OF THE STEM OF THE PROSTHESIS.

The mean and standard deviation of the co-ordinates of the centre of the head are tabled in table 6.7.

The standard deviations in determining the three co-ordinates of the centre of the head of the prosthesis range from 0.29 mm for the *x* co-ordinate, 0.08 mm for the *y* co-ordinate to 0.47 mm for the *z* co-ordinate.

	CO-ORDINATES OF THE CENTRE OF THE HEAD		
MEASUREMENT	**X (mm)**	**Y (mm)**	**Z (mm)**
1	260.80	211.10	216.00
2	260.20	211.00	216.70
3	260.60	211.00	215.70
4	260.10	211.10	216.70
5	260.40	210.90	215.90
MEAN (mm)	260.42	211.02	216.20
STD. DEV'N	0.29	0.08	0.47

Table 6.7. The standard deviation of five measurements of the centre of the head of the prosthesis.

The results of five independent measurements of the co-ordinates of the tip of a hemispherical prosthesis are tabled in table 6.8.

The results show a standard deviation ranging from 0.16 mm to 0.19 mm for the three co-ordinates.

	CO-ORDINATES OF THE TIP		
MEASUREMENT	**X (mm)**	**Y (mm)**	**Z (mm)**
1	316.00	76.00	230.40
2	316.30	76.20	230.00
3	316.40	76.30	230.00
4	316.20	76.10	230.20
5	316.50	76.40	230.10
MEAN (mm)	316.28	76.20	230.14
STD. DEV'N	0.19	0.16	0.17

Table 6.8. The standard deviation of five measurements of the tip of the prosthesis.

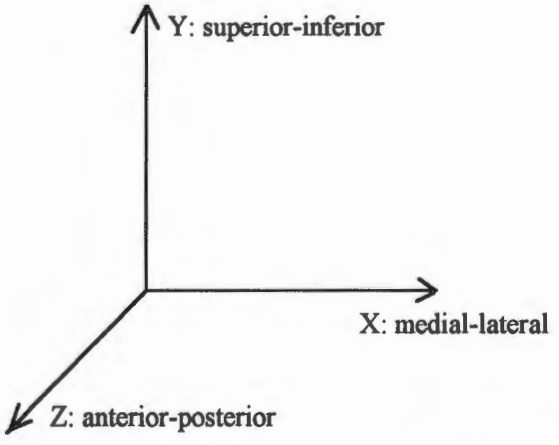

Figure 6.1 The co-ordinate axes indicated in the results

6.5 EVALUATION OF A SIMULATED PATIENT FOLLOW-UP

The results of the determination of the accuracy in co-ordinating the beads is tabled in tables 6.9 a-d, the distance between the head and the tip on three sets in table 6.10 and the calculated distances between the beads in table 6.11. CT1-3 refer to the three successive stereo-pairs of the same specimen.

STEREO-PAIR NUMBER	CO-ORDINATE X_1	CO-ORDINATE Y_1	CO-ORDINATE Z_1
CT1	296.9	199.4	157.0
CT2	297.0	199.5	157.0
CT3	296.9	199.6	156.9
MEAN	296.9	199.5	156.9
STD DEV'N	0.06	0.10	0.06

Table 6.9a. Comparison of the co-ordinates for bead number 1

STEREO-PAIR NUMBER	CO-ORDINATE X_2	CO-ORDINATE Y_2	CO-ORDINATE Z_2
CT1	324.2	167.4	172.1
CT2	324.3	167.1	171.6
CT3	324.2	167.1	172.2
MEAN	234.2	167.2	172.0
STD DEV'N	0.06	0.17	0.32

Table 6.9b. Comparison of the co-ordinates for bead number 2

STEREO-PAIR NUMBER	CO-ORDINATE X_3	CO-ORDINATE Y_3	CO-ORDINATE Z_3
CT1	321.7	156.5	165.1
CT2	321.3	156.5	165.8
CT3	321.6	156.7	165.0
MEAN	321.5	156.6	165.3
STD DEV'N	0.21	0.12	0.44

Table 6.9c. Comparison of the co-ordinates for bead number 3

STEREO-PAIR NUMBER	CO-ORDINATE X_4	CO-ORDINATE Y_4	CO-ORDINATE Z_4
CT1	295.5	75.4	178.5
CT2	295.7	75.6	178.4
CT3	295.5	75.3	178.6
MEAN	295.6	75.4	178.5
STD DEV'N	0.12	0.15	0.10

Table 6.9d. Comparison of the co-ordinates for bead number 4

	DISTANCE MEASUREMENT (mm)			MEAN (mm)	STD DEV'N
	CT1	CT2	CT3		
HEAD TO TIP	155.0	154.7	155.0	154.9	0.17

Table 6.10. Comparison of the calculated distances between the centre of head and the tip of the stem for the three x-ray pairs.

BEAD NUMBERS	DISTANCE MEASUREMENT (mm)			DIFFERENCE CT1-CT2 (mm)	DIFFERENCE CT1-CT3 (mm)
	CT1	CT2	CT3		
1 & 2	44.69	44.83	45.12	0.14	0.43
1 & 3	50.21	50.14	50.19	-0.07	-0.02
1 & 4	125.86	125.73	126.23	-0.13	0.38
2 & 3	13.19	12.44	12.95	-0.75	-0.25
2 & 4	96.58	96.12	96.43	-0.47	-0.16
3 & 4	86.27	85.82	86.59	-0.45	0.32
MEAN OF DIFFERENCES (mm)				0.34	0.26
STANDARD DEVIATION OF THE DIFFERENCES				0.49	0.35

Table 6.11. Comparison of the calculated distances between the implanted beads for the three x-ray pairs.

The results shown that the standard deviations in co-ordinating the same point on the sucessive x-rays range between 0.06 and 0.44 mm, with the largest deviations being in the *z* co-ordinate. The standard deviation for determining the distance between points on the successive x-rays as compared to the first set was 0.49 mm and 0.35 mm.

Tables 6.12 and 6.13 compare the distances between the beads and the centre of the head and the beads and the tip of the stem, respectively for a second group of x-rays of a specimen.

BEAD NUMBER	3-D DISTANCE TO CENTRE OF HEAD (mm)		DIFFERENCE (mm)
	SET 1	SET 2	
1	85.9	82.9	3.0
2	71.1	68.4	2.7
3	68.8	66.5	2.3
4	41.1	37.9	3.2

Table 6.12. Comparison between the beads and the centre of the head in a subsidence test.

BEAD NUMBER	3-D DISTANCE TO TIP OF THE STEM (mm)		DIFFERENCE (mm)
	SET 1	SET 2	
1	74.6	77.7	-3.1
2	94.1	97.5	-3.4
3	110.4	113.9	-3.5
4	108.3	111.5	-3.2

Table 6.13. Comparison between the beads and the tip of the stem in a subsidence test.

A combination of the data shown in tables 6.12 and 6.13 together with data similar to that shown in tables 6.9 to 6.11 allows a calculation of the overall movement of the prosthesis. The overall movement for the bone-specimen described above is shown in table 6.14.

Head 1 to Head 2 refers to the distance the centre of the head of the prosthesis moved on the successive x-rays. Similarly Tip 1 to Tip 2 refers to the distance moved by the tip of the prosthesis

POSITION	DISTANCE (mm)
HEAD 1 TO HEAD 2	3.3
TIP 1 TO TIP 2	3.4

Table 6.14. Overall movement of a test specimen.

The combined results for tables 6.12 to 6.14 indicate a movement of 3 mm.

CHAPTER 7
DISCUSSION

The implementation of Roentgen Stereophotogammetric Analysis (RSA) in the detection of migration and subsidence in total hip arthroplasty has been shown to be capable of measuring the position of implanted markers with accuracies of between 0.2 mm and 0.8 mm. With accuracies of these magnitudes, RSA should become a routine clinical tool in the orthopaedic practice. One of the primary development considerations should be to find a system that is simple to install and operate, cost effective and which produces accurate and meaningful results.

The basic requirements for an orthopaedic RSA system are the production of a stereo-pair of x-rays with the subject in the same orientation, a calibration system in order to determine the parameters of the x-ray tube and internal reference beads positioned in the bone.

The production of the stereo-pairs is the requirement which is the most varied in the five previously described systems. Simultaneous exposure of the subject by two x-ray tubes is the most effective and accurate method of producing the stereo-pairs, but has the disadvantages of inaccessibility due to the requirements of having two x-ray sources in the same room and the possibility of image degradation due to the scatter from one source-film unit affecting the second film. Four of the five systems use two synchronised x-ray sources to produce the stereo-pairs (Turner-Smith *et al.* 1990, Selvik *et al.* 1983, Green *et al.* 1983, Lippert *et al.* 1982). The fifth system described by Chafetz *et al.* (1984) uses a single x-ray source which is moved vertically between exposures. Patient movement between exposures is a reported source of inaccuracies in the measurements (Chafetz *et al.* 1985).

Our system, however, while using only one x-ray source makes use of the video cameras to detect the rotation of the patient on the turn-table thus enable the mathematical rotation

of the patient back into the first system. This also means that any other movements of the patient may be detected and corrected for. This system operates successfully as long as the external marker bars are positioned in such a way that they move with the femur as a rigid body. Independent movement of the markers introduce errors in the calculations. The fixed x-ray source allows the use of a built in "Bucky" stand to improve the quality of the x-rays, and ensure rapid cassette changing. Repositioning the patient by rotating him/her on the turn-table is a simple and a quick procedure using the graduations marked for the braking handle.

The calibration systems for the five methods described, as well as for our system, are all essentially a frame of some description, of which points, with known spatial positions, are imaged on the x-rays. The calibration points are essential for the mathematical location of the x-ray source(s). The frames vary in design and construction, eg. the frame used in the Oxford system consists of two plates of light weight material onto which accurately milled grids are imposed and filled with two different radiopaque materials (Turner-Smith 1990). The Lund frame has accurately positioned fiducial markers in the back plane of the frame and reference markers in the front plane. Accurately constructed frames with known spatial positions of the reference markers with respect to each other are used by the Cleveland and the San Francisco systems. The calibration system in Seattle consists of engraved crosses and markers, is co-ordinated after construction and thus a high degree of precision is not essential in the construction phase. This is the case for our system. The intersections of the wires form the reference points and are clearly visible on the x-rays without obscuring vital information regarding the implant. An added advantage is that all the intersections may be digitised as those obscured by the prosthesis are determined by extrapolating the visible wires.

The internal reference markers are similar in all the systems, with metallic beads being implanted into the bone surrounding the prostheses during the surgical procedure. One or two reference points are determined on the prosthesis in all the systems except for the system developed in Cleveland. In this system the reference points are beads positioned in

the cement mantle. The accurate redetermination of the reference points is essential for the determination of the position of the prosthesis on successive x-rays. The determination of the centre of the head of the prosthesis has been shown to be a reliable and accurate reference point as is demonstrated by the deviations from a mean of five independent measurements of 0.29 mm for the x co-ordinate, 0.08 mm for the y co-ordinate and 0.47 mm for the z co-ordinate. The relatively large error in the z co-ordinate is due to the error in the coincidence of the centre of the ellipse (the image of the projection of the sphere on the film) and the centre of the sphere (the actual object) in the z, or antereo-posterior, direction. The calibration frame constrains the antereo-posterior position of the patient to a small degree and thus a relatively constant error results and no computational adjustments need to be made.

The determination of a second reference point on the distal section of the prosthesis provides a verification of any movement detected using the proximal reference point. The determination of the tip of the stem as the second reference point for our study using second order polynomials, was accurate for the hemispherical tips but, the semi-flat tipped stems did not indicate as good an accuracy as would be expected due to the lack of a definite turning point. The accuracies were, however, acceptable as the determination of the distance between the centre of the head and the "tip" of the stem of a "flat" tipped prosthesis showed the deviation from a mean of three results for the simulated follow-up to be 0.17 mm.

The data capture phase of our system requires approximately 20 minutes to position and focus the cameras and to capture the images of the "empty" control frame. This need only be done once if the set-up is to remain in a permanent position. The image capture phase involving the patient is fast requiring only the change over of x-ray film cassettes and the rotation of the patient between exposing of the x-rays. The x-ray exposures used are the same as would be used for routine clinical x-rays. The digitising and calculation phases took approximately 45 minutes for the first patient in a set and thereafter 15 minutes per

patient. The clinician would thus have accurate information as to the position of a prosthesis within 20 minutes of the x-ray being exposed.

The evaluation of our system has indicated that the accuracy achieved in the co-ordination of beads is 0.21 mm or less over a range of ± 20 mm in the three dimensions. The mean difference of 0.24 mm, when calculating the distances between the beads using the results from the reflex microscope as an assumed error free control, indicate that the system is capable of detecting and measuring subsidence up to 0.3 mm in three dimensions in the dry bone specimens.

The mean difference of 0.14 mm over a range of ± 30 mm, in the determination of distances between five beads by two independent observers, has been demonstrated. The magnitude of the differences indicates that meaningful results may be obtained if different observers do the follow-up analyses on the patients. This finding is supported by the intraobserver repeatability evaluations. Mean standard deviations in the repeated measurement of distances between a series of beads was found to be between 0.13 and 0.16 mm with the largest deviation being 0.33 mm. This would indicate the capabilities of measuring the distance between two beads on successive x-rays to an accuracy better than 0.3 mm.

In the simulated "patient follow-up" study to determine the accuracies of co-ordinating the common beads, standard deviations of between 0.06 mm and 0.44 mm from the mean of the co-ordinates for the four common beads in the three sets of stereo pairs were observed. Translating the co-ordinates into distance measurements between the beads, resulted in mean differences from the control set stereo pair of 0.34 mm for the second stereo pair and 0.26 mm for the third pair. This again qualifies the capability of the system to determine the position of a bead with an accuracy of 0.3 mm on successive sets of stereo pairs of x-rays.

The subsidence test in the simulated "patient follow-up" resulted in a overall subsidence of the prosthesis of ±3.4 mm in three dimensions. The differences between the calculated 3-D distances from the beads to the centre of the head of the prosthesis ranged from 2.3 mm

to 3.2 mm and those from the beads to the tip of the stem ranged from 3.1 mm to 3.5 mm. The calculated differences in the 3-D distances thus agree with the calculated overall difference from the initial position and confirm that the prosthesis in the test specimen subsided by an amount of between 2.3 mm and 3.5 mm in all three dimensions.

A subsidence of 3 mm may be considered a gross movement while in the majority of cases in orthopaedic practice the detection of subsidence of much smaller magnitudes is desirable. However, due to the nature of the dry bones small movements were difficult to simulate.

In our experience with the initiation of the patient studies it was found that the most critical aspect was the positioning and securing of the external markers. Careful checking of their position on the video images for both rotated positions was essential to ensure sufficient common points were visible in order to mathematically perform the rotations.

It is believed that the system will be of great value to orthopaedic surgeons in clinical situations where two x-ray sources with simultaneous firing control are unavailable. The accuracies determined in this study indicate implementation in routine clinical practice will provide valuable information regarding the position of the prosthesis.

CHAPTER 8

CONCLUSIONS AND RECOMMENDATIONS FOR FUTURE DEVELOPMENTS

The aim of this study, namely to develop a Roentgen Stereophotogrammetric Analysis system to measure the subsidence of the femoral component in total hip arthroplasty, has been realised.

CONCLUSIONS:

Addressing the objectives the following are concluded:

i) a RSA system using an x-ray photogrammetric system and a close range video stereophotogrammetric system has been developed;

ii) the hardware for clinical trials was built and implemented in the clinical setting for the *in-vitro* evaluations;

iii) the accuracy of the system was evaluated and found to be capable of measuring subsidence of 0.3 mm;

iv) clinical trials were initiated and the hardware was evaluated with reference to the patient.

FUTURE DEVELOPMENTS:

Future developments of this study should include:

i) the routine use of the system in an orthopaedic centre to monitor patients with implanted beads on a long term basis;

ii) the development of a structure to support the external markers securely and comfortably

iii) the refinement of the calculation of the tip of the stem to determine a reference point on a flat tipped femoral component;

iv) the development of an automated video digitising system (already in progress);

v) the development of methods to ascertain possible rotations of the prosthesis and adapting the system to analyse other total joint arthroplasties, for example total knee replacements (already in progress).

REFERENCES

Abdel-Dayem HM, Barodawala YK, Papademetriou T

1982

Scintigraphic arthography, comparison with contrast arthography and future applications.

Clinics in Nuclear Medicine 7:516-522

Adams LP

1981

X-ray stereo photogrammetry locating the precise, three dimensional position of image points.

Medical and Biological Engineering and Computing 19:569-578

Adams LP and Wilding RJC

1988

A stereometric technique for measuring residual alveolar ridge volumes.

Journal of Prosthetic Dentistry 60(3):388-393

Adams LP and Wilding RJC

1988

Tooth wear measurements using a reflex microscope.

Journal of Oral Rehabilitation 15:605-613

Amstutz HC, Ouzounian T, Grauer D, Flink C, Kirkpatrick J, Bassett L

1986

The grid radiograph: A simple technique for consistent high-resolution visualisation of the hip.

Journal of Bone and Joint Surgery 68-A:1052-1056

Angoletto EB, Pagani M

1974

X-ray photogrammetry with special reference to the treatment of uterine cancer.

Proceedings of the Biostereometrics '74 Symposium Washington DC:409-435

Aronson AS, Holst L, Selvik G.

1974

An instrument for insertion of radiopaque bone markers.

Radiology 113:733-734

Ateshian GA, Soslowsky LJ, Mow VC

1991

Quantitation of articular surface topography and cartilage thickness in knee joints using stereophotogrammetry.

Journal of Biomechanics 24:761-776

Baldursson H, Egund N, Hansson LI, Selvik G

1979

Instability and wear of total hip prostheses determined with roentgen stereophotogrammetry.

Archives of Orthopaedic and Traumatic Surgery 95:257-263

Baldursson H, Hansson LI, Olsson TH, Selvik G

1980

Migration of acetabular socket after total hip replacement determined with roentgen stereophotogrammetry.

Acta Orthopaedica Scandinavica 51:535-540

Baumrind S

1975

A system for craniofacial mapping through the intergration of data from stero x-ray films and stero photographs.

Proceedings of the ASP Symposium on Close-Range Photogrammetric systems Illinois:142-166

Beckenbaugh RD, Ilstrup DM

1978

Total hip arthroplasty: A review of 333 cases with long term follow-up.

Journal of Bone and Joint Surgery 60A:306-313

Brand RA, Yoder SA, Pederson DR

1985

Inter observer variability in interpreting radiographic lucencies about total hip replacements.

Clinical Orthopaedics and Related Research 192:237-239

Brand RA, Pederson DR, Yoder AY

1986

How definition of "loosening" affects the incidence of loose total hip reconstructions.

Clinical Orthopaedics and Related Research 210:185-191

Brown RH, Burstein AH, Nash Cl, Schock CC

1976

Spinal analysis using a three-dimensional radiographic technique.

Journal of Biomechanics 9:355-365

Chafetz N, Baumrind DDS, Murray WR, Genant HK

1984

Femoral prosthesis subsidence in asymptomatic patients: A stereophotogrammetric assessment..

Investigative Radiology 19:235-241

Chafetz N, Baumrind S, Murray WR, Genant HK, Korn EL.

1985

Subsidence of the femoral prosthesis:A stereophotogrammetric analysis.

Clinical Orthopaedics and Related Research 201:60-67

Charnley JC

1965

A biomechanical analysis of the use of cement to anchor the femoral head prosthesis.

Journal of Bone and Joint Surgery 47B:354-363

Charnley JC, Cupic Z

1973

The nine and ten year results of low-friction arthroplasty of the hip.

Clinical Orthopaedics and Related Research 95:9-25

Cotterill P, Hunter GA, Tile M

1982

A radiographic analysis of 166 Charnley-Muller total hip arthroplasties.

Clinical Orthopaedics and Related Research 163:120-126

Cupic Z

1979

Long-term follow-up of Charnley arthroplasties of the hip.

Clinical Orthopaedics and Related Research 141:28-43

Dall DM, Learmonth ID, Solomon M, Davenport M

1992

Long-term results of Charnley low-friction arthroplasty of the hip

South African Journal of Surgery 30:171-174

Davy DT, Kotzar GM, Brown RH, Heiple KG, Goldberg VM, Berilla J, Burstein AH.

1988

Telemetric force measurements across the hip after total hip arthroplasty.

Journal of Bone and Joint Surgery. 70A:45-50

Djerf K, Edholm P, Hedbrant J

1987

A simplified roentgen stereophotogrammetric method

Acta Radiologica 28:603-606

Feith R

1975

Side-effects of acrylic cement implanted into bone: a histological, (micro)angiographic, fluorescence-microscopic and autoradiographic study in the rabbit femur.

Acta Orthopaedica Scandinavica Supplementum 161

Freiberger RH

1986

Evaluation of hip prostheses by imaging methods.

Seminars in Roentgenology 21:20-28

Fowles JV

1985

Skeletal trauma notes

Ch 2. Baltimore: Williams and Wilkins

Gelman MI, Coleman RE, Stevens PM, Davey BW

1978

Radiography,radionuclide imaging and arthography in the evaluation of total hip and knee replacement.

Nuclear Medicine 128:677-682

Gold BL, Walker PS

1974

Variables affecting the friction and wear of metal-on-plastic total hip joints.

Clinical Orthopaedics and Related Research 100:270-278

Goldring SR, Schiller AL, Roelke M et al.

1983

The synovial like membrane at the bone-cement interface in loose total hip replacements and its proposed role in bone lysis.

Journal of Bone and Joint Surgery 65A:575-584

Green DL, Bahniuk E, Leibelt RA, Fender E, Mirkov P

1983

Biplane radiographic measurements of reversible displacement (including clinical loosening) and migration of total joint replacements.

Journal of Bone and Joint Surgery 65A:1134-1143

Gruen TA, McNeice GM, Amstutz HC

1979

"Modes of failure" of cemented stem-type femoral components: A radiographic analysis of loosening.

Clinical Orthopaedics and Related Research 141:17-27

Gudmundsson GH, Hedeboe J, Kjaer J.

1985

Mechanical loosening after hip replacement

Acta Orthopaedica Scandinavica 56:314-317

Hallert B

1970

X-ray photogrammetry

p1-2, Amsterdam: Elsevier Publishing Company

Hardinge K, Porter ML, Jones PR, Hukins DWL, Taylor CJ

1991

Measurement of hip prostheses using image analysis.

Journal of Bone and Joint Surgery 73B:724-728

Harris WH, McCarthy JC, O,Neill DA

1982

Femoral component Loosening using contempory techniques of femoral cement fixation.

Journal of Bone and Joint Surgery 64A:1063-1067

Huiskes R

1980

Some fundamental aspects of human joint replacement: analyses of stresses and heat conduction in bone-prosthesis structures.

Acta Orthopaedica Scandinavica Supplementum 185

Hunter JC, Baumrind S, Genant HK, Murray WR, Ross SE

1979

The detection of loosening in total hip arthroplasty: Description of a stereophotogrammetric computer assisted method.

Investigative Radiology 14:323-329

Jakim I, Barlin C, Sweet MBE

1989

Radiological signs of loosening of the femoral stem in cementless THA.

South African Journal of Surgery 27:78-83

Jasty M, Maloney WJ, Bragdon CR, O'Connor DO, Haire T, Harris WH

1991

The initiation of failure in cemented femoral components of hip arthroplasties.

Journal of Bone and Joint Surgery 73B:551-558

Johanson NA, Bullough PG, Wilson PD et al.

1987

The microscopic anatomy of the bone-cement interface in failed total hip arthroplasties.

Clinical Orthopaedics and Related Research 218:123-135

Johnston RC, Crownshield RD

1983

Roentgenologic results of total hip arthroplasty: A ten year follow-up study.

Clinical Orthopaedics and Related Research 181:92-98

Johnston RC, Fitzgerald RH, Harris WH, Poss R, Muller ME, Sledge CB

1990

Clinical and radiographic evaluation of total hip replacement:A standard system of terminology for reporting results.

Journal of Bone and Joint Surgery 72-A:161-168

Jonason C, Hindmarsh J

1975

Stereo x-ray photogrammetry as a tool in studying scoliosis.

Proceeding of ASP Symposium on Close-Range Photogrammetry, Illinois 245-259

Jones PR, Taylor CJ, Hukins DWL, Hardinge K, Porter ML

1988

Prosthetic hip failure: preliminary findings of retropespective radiograph image analysis.

Engineering in Medicine 17:119-125

Jones PR, Taylor CJ, Hukins DWL, Hardinge K, Porter ML

1989

Prosthetic hip failure: retropespective radiograph image analysis of the acetabular cup.

Journal of Biomedical Engineering 11:253-257

Karara HM

1979

Non-topographic photogrammetry: X-ray systems and applications

pp.846-857 In: Slama CC editor-in-chief. Manual of Photogrammetry 4th Ed.

Virginia: American Society for Photogrammetry and Remote Sensing

Kärrholm J

1989

Roentgen stereophotogrammetry: Review of orthopedic applications.

Acta Orthopaedica Scandinavica 60:491-503

Kerr G, Turner-Smith A, White S, Rosenstein A, Cunningham J

1991

Prosthetic joint loosening: non-radiographic methods.

Oxford Orthopaedic Enginneering Centre Annual Report 18:3-4

Klein F

1908

Elementary mathematics from an advanced standpoint. Geometry. Translated from German 1939.

New York: Dover Publications

Kratky V

1975

Analytical x-ray photogrammetry in scoliosis.

Proceedings of the ASP Symposium on Close-Range Photogrammetric Systems Illinois:167-185

Learmonth ID, Dall DM, Solomon M, Heywood AWB

1991

A comparison of the results of Charnley low-friction arthroplasty in rheumatoid arthritis and osteoarthritis.

Journal of Orthopaedic Rheumatology 4:47-55

Lennox DW, Schofield BH, McDonald DF, Riley LH

1987

A histological comparison of aseptic loosening of cemented, press-fit, and biological ingrowth prostheses.

Clinical Orthopaedics and Related Research 225:171-191

Linder L, Lindberg L, Carlsson Å

1983

Aseptic loosening of hip prostheses: a histological and enzyme histochemical study.

Clinical Orthopaedics and Related Research 175:93-104

Ling RSM

1986

Observations on the fixation of implants to the bony skeleton.

Clinical orthopaedics and related research 210:80-98

Lippert FG, Harrington RM, Veress SA, Fraser C, Green D, Bahniuk E

1982

A comparison of convergent and bi-plan x-ray photogrammetric systems used to detect total joint loosening.

Journal of Biomechanics 15:677-682

McBeath AA, Foltz RN

1979

Femoral component loosening after total hip arthroplasty.

Clinical Orthopaedics and related research 141:66-70

McCoy TH, Salvati EA, Ranawat CS, Wilson PD

1988

A fifteen year follow-up study of one hundred Charnley low-friction arthroplasties.

Orthopaedic Clinics of North America 19:467-476

McNeil GT

1966

X-ray stereophotogrammetry

Photogrammetric Engineering 32(6):993-1004

Mehlhoff MA, Sledge CB

1990

Comparison of cemented and cementless hip and knee replacements.

Arthritis and Rheumatism 33:293-297

Mjöberg B

1986

Loosening of the cemented hip prosthesis: The importance of heat injury.

Acta Orthopaedica Scandinavica Supplementum 221:1-40

Mjöberg B, Brismar J, Hansson L, Petterson H, Selvik G, Onnerfalt R.

1985

Definition of endoprosthetic loosening: Comparison of arthrography, scintigraphy and roentgen stereophotogrammetry in prosthetic hips.

Acta Orthopaedica Scandinavica 56:469-473

Moffit FH

1972

Stereo x-ray photogrammetry applied to orthodontic measurements

International Archives of Photogrammetry 19:1-16

Morscher EW

1983

Cementless total hip arthroplasty

Clinical Orthopaedics and related research 181:76-91

Mulroy RD, Sedlacek RC, O'Connor DO, Estok 11 DM, Harris WH

1991

Technique to detect migration of femoral components of total hip arthroplasties on conventional radiographs.

Journal of Arthroplasty 6(suppl):S1-S4

Munuera L, Garcia-Cimbrelo E

1990

The femoral component in low-friction arthroplasty after ten years

Clinical Orthopaedics and Related Research 279:163-175

Murray WR, Rodrigo JJ

1975

Arthography for assessment of pain after total hip replacement. A comparison of arthographic finding in patients with and without pain.

Journal of Bone and Joint Surgery 57A:1060-1065

Nilsson KG, Kärrholm J, Ekelund L, Magnusson P.

1991

Evaluation of micromotion in cemented vs uncemented knee arthroplasty in osteoarthritis and rheumatoid arthritis.

Journal of Arthroplasty 6:265-278

O'Neill DA, Harris WH

1984

Failed total hip replacements: assessment by plain radiography, arthrograms, and aspiration of the hip joint.

Journal of Bone and Joint Surgery 66A: 540-546

Paterson M, Fulford P, Denham R

1986

Loosening of the femoral component after total hip replacement. The thin black line and the sinking hip.

Journal of Bone and Joint Surgery 68B:392-397

Pellicci PM, Salvati EA, Robinson HJ

1979

Mechanical failures in total hip replacement requiring reoperation.

Journal of Bone and Joint Surgery 61A:28-36

Pillar RM, Lee JM, Maniatopoulos C

1986

Observations on the effect of movement on bone ingrowth into porous-surfaced implants.

Clinical orthopaedics and Related Research 208:108-113

Poss R., Walker P., Spector M., Reilly DT., Robertson DD., Sledge CB.

1988

Strategies for improving fixation of femoral components in total hip arthroplasty.

Clinical Orthopaedics and Related Research 235:181-194

Radin EL, Rubin CT, Thrasher EL et al.

1982

Changes in the bone-cement interface after total hip replacement. An in vivo animal study.

Journal of Bone and Joint Surgery 64A:1188-1200

Rhinelander FW, Nelson Cl, Stewart RD, Stewart CL

1979

Experimental reaming of the proximal femur and acrylic cement implantation. Vascular and histological effects.

Clinical Orthopaedics and Related Research 141:74-89

Rosenstein AD, McCoy GF, Cunningham JL, McLardy-Smith PD, Bulstrode CJ, Turner-Smith AR

1989

The differentiation of loose and secure femoral implants in total hip replacement using a vibrational technique.

Journal of Engineering in Medicine:Proceedings of the Institution of Mechanical Engineers 203(H2):77-81

Rothman RH, Cohn JC

1990

Cemented versus cementless totalm hip arthroplasty: A critical review.

Clinical Orthopaedics and Related Research 254:153-169

Rushton N, Coakley AJ, Tudor J,Wraight EP

1982

The value of Technetium and Gallium scanning in assessing pain after total hip replacement.

Journal of Bone and Joint Surgery 64B:313-318

Ryd L

1986

Micromotion in knee arthroplasty: A Roentgen stereophotogrammetric analysis of the tibial component fixation.

Acta Orthopaedica Scandinavica Supplementum 220:1-80

Ryd L, Toksvig-Larsen S

1993

Early postoperative fixation of tibial components: An *in vivo* roentgen stereophotogrammetric analysis.

Journal of Orthopaedic Research 11:142-148

Salvati EA, Freiberger RH, Wilson PD

1971

Arthography for complications of total hip replacement. A review of thirty one arthrograms.

Journal of Bone and Joint Surgery 53A:701-709

Schneider R, Freiberger RH, Ghelmaan B, Ranawat CS

1982

Radiologic evaluation of painful joint prostheses.

Clinical Orthopaedics and Related Research 170:156-168

Selvik G, Alberius P, Aronson AS.

1983

A Roentgen stereophotogrammetric system: Construction, calibration and technical accuracy.

Acta Radiologica Diagnosis 24:343-352

Sevitt

1981

Bone repair and fracture healing in man

pp. 41-52

New York: Churchill Livingstone (Current Problems in Orthopaedics)

Slooff T

1971

The influence of acrylic cement. An experimental study.

Acta Orthopaedica Scandinavica 42:465-481

Snorrason F, Kärrholm J.

1990

Early loosening of revision hip arthroplasty; A Roentgen stereophotogrammetric analysis.

Journal of Arthroplasty 5:217-229

Stauffer RN

1982

Ten year follow-up study of total hip replacement.

Journal of Bone and Joint Surgery 64A:983-990

Sturesson B, Selvik G, Uden A

1989

Movements of the sacroiliac joints: A Roentgen stereophotogrammetric analysis.

Spine 14:162-165

Sund G, Rosenqvist J

1983

Morphological changes in bone following intramedullary implantation of methyl methacrylate. Effects of medullary occlusion. A morphometrical study.

Acta Orthopaedica Scandinavica 54:148-156

Sutherland CJ, Wilde AH, Borden LS, Marks KE

1982

A ten year follow-up of 100 consecutive Muller curved-stem total hip replacement arthroplasties.

Journal of Bone and Joint Surgery 64A:970-982

Thompson EH

1969

An introduction to the algebra of matrices with some applications

p. 142, London: Adam Hilger

Turner-Smith AR

1990

X-ray photogrammetry of artificial joints.

Photogrammetric Record 13:347-366

Turner-Smith AR, White SP, Bulstrode C

1990

X-ray photogrammetry of artificial hip joints

1395:587-594 In: Proceedings of SPIE; Close-range Photogrammetry Meets Machine Vision.

Washington: SPIE

Uri G, Wellman H, Capello W, Robb J, Greenman G

1984

Scintigraphic and x-ray arthographic diagnosis of femoral prosthesis loosening.

Journal of Nuclear Medicine 25:661-663

Veress SA, Lippert FG, Takamoto T

1977

An analytical approach to x-ray stereophotogrammetry.

Photogrammetric Engineering and Remote Sensing 43: 1503-1510

Veress SA

1989

X-ray Photogrammetry, Systems, and Applications.

pp.167-186 In: Karara HM ed. Non-Topographic Photogrammetry 2ed.

Virginia: American Society for Photogrammetry and Remote Sensing.

Walker PS, Sathasivam S

1992

A simplified radiographic method for measuring bone-component motion in total knees

Journal of Biomechanics 25:1059-1066

Weiner R, Hoffer PB, Thakur ML

1981

Lactoferrin: its role as a Ga-67 binding protein in polymorphonuclear leukocytes

Journal of Nuclear Medicine 22:32-37

Weiss PE, Mall JC, Hoffer PB, Murray WR, Rodrigo JJ, Genant HK

1979

^{99m}Tc-methylene diphosphonate bone imaging in the evaluation of total hip prostheses

Journal of Nuclear Medicine 133:727-730

Whiteside LA, Easley JC

1989

The effect of a collar and distal stem fixation on micromotion of the femoral stem in uncemented total hip arthroplasty.

Clinical Orthopaedics and Related Research 239:145-153

Willert HG, Ludwig J, Semlitsch M

1974

Reactions of bone to methacrylate after hip arthroplasty. A long-term gross, light microscopic and scanning electron microscopic study.

Journal of Bone and Joint Surgery 56A:1368-1382

Wroblewski BM

1986

!5-21 year results of the Charnley low-friction arthroplasty

Clinical Orthopaedics and Related Research 211:30-35

Wykman A, Olsson E, Axdorph G, Goldie I

1991

Total hip arthroplasty.

Journal of Arthroplasty 6(1):19-29

APPENDIX A

DETERMINATION OF THE CENTRE OF THE HEAD OF THE PROSTHESIS

In order to determine whether the femoral component of a total hip replacement has subsided it is necessary to establish reference points on the prosthesis itself. Selecting a standard feature common to the all types of prostheses as this reference point ensures that the overall RSA system may be used with modification on range of different components.

The head of a metal prosthesis has been found to be spherical with an out-of-roundness of less than 5 μm (Gold and Walker 1974). Baldursson *et al.* (1979) established a method whereby points around the circumference of the head of the prosthesis were measured on both x-ray films and the centre of the head calculated.

The central projection of a sphere or a circle on a plane is a conic section and combined with the angles of projection used in radiography the section appears as an ellipse.

An ellipse may be determined from five points on the circumference and represented by the following second-degree equation:

$$a_{11}x^2 + 2a_{12}xy + a_{22}y^2 + 2a_{13}x + 2a_{23y} + 1 = 0 \qquad (1)$$

The five points on the circumference determine the coefficients a_{11},.....a_{23} and the centre of the ellipse is determined by

$$x_0 = -\frac{1}{D}(a_{13}a_{22} - a_{12}a_{23}) \quad y_0 = -\frac{1}{D}(a_{11}a_{23} - a_{12}a_{13}) \qquad (2)$$

where $D = a_{11}a_{22} - a_{12}^2$

These equations calculate the centre of the ellipse which differs from the centre of the sphere by Δx as is shown in figure A.1.

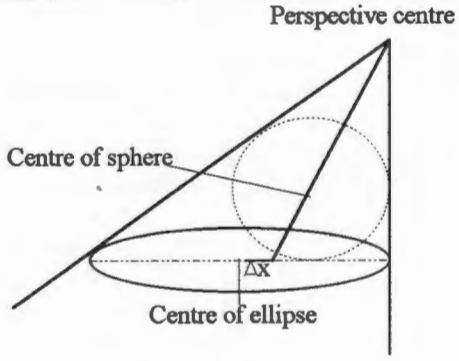

Figure A.1. The difference Δx between the centre of the sphere and the centre of the ellipse on the central projection of a sphere on a plane. (Adapted from Baldursson *et al.* 1979).

McNeil (1966) used trigonometry to derive a formula to calculate this difference .

$$\Delta x = \frac{c}{2}\tan(\theta - \phi) + \tan(\theta + \phi) - 2\tan\theta \qquad (3)$$

c : distance from the focus to the image

θ : angle between the perpendicular to the image and the centre of the sphere

ϕ : angle of the radius of the sphere as seen from the focus

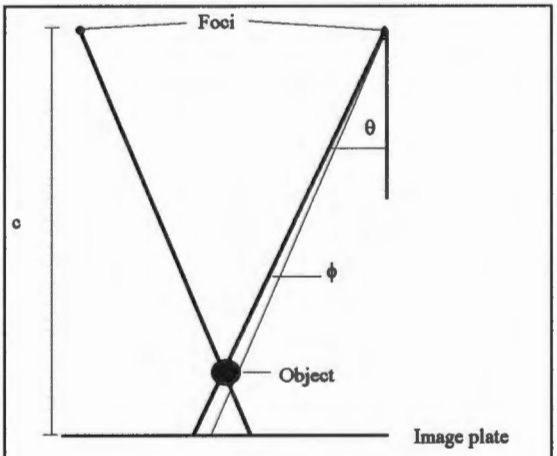

Figure A.2 An illustration of the geometry used to calculate the distance Δx. (Adapted from Baldursson *et al.* 1979)

Baldursson *et al.* (1979) found the values Δx = 0.138 mm and Δx = 0.055 mm for two different prostheses. If the centre of the sphere lies symmetrically between the two foci Δx will have the same magnitude but opposite direction and therefore not affect the calculated position of the centre in the x-direction. Errors do, however, occur in the calculated y and z co-ordinates. Selvik (1974), calculated the errors as follows:

$$dz = \frac{h^2}{bc}dx^1 \qquad dy = \frac{yh}{bc}dx^1 \qquad (4)$$

where b: distance between the foci

c: distance from the foci to the fiducial marks

h: perpendicular distance from the sphere to line joining the foci

y: image y co-ordinate

dx^1: $= 2\Delta x$.

Values for Δy in the same study were 0.018 mm and 0.007 mm. It was concluded that the geometric errors in the coincidence of the centre of the ellipse and the centre of the sphere are unimportant except in the z-direction (dz between 0.137 and 0.344 mm). Positioning the patient in approximately the same position in successive x-rays will result in a constant error and thus computational adjustments are not required.

APPENDIX B
PROJECTIVE TRANSFORMATIONS

Since the picture is a special case of central projection it is possible to make use of central projection geometry and in particular the mathematics of projective transformations when image co-ordinates are measured in the plane of the picture.

ANALYTICAL DEFINITION OF THE PROJECTIVE TRANSFORMATION

It may be stated that (Klein 1908):

$$X' = \frac{a_{11}X + a_{12}Y + a_{13}Z + a_{14}}{a_{41}X + a_{42}Y + a_{43}Z + a_{44}}$$

$$Y' = \frac{a_{21}X + a_{22}Y + a_{23}Z + a_{24}}{a_{41}X + a_{42}Y + a_{43}Z + a_{44}} \qquad (1)$$

$$Z' = \frac{a_{31}X + a_{32}Y + a_{33}Z + a_{34}}{a_{41}X + a_{42}Y + a_{43}Z + a_{44}}$$

where a_{11}-a_{41} represent the four by four matrix determining the transformation parameters for transforming three-dimensions into three-dimensions.

That is to every point X,Y,Z, there corresponds a definite point X', Y', Z', provided only that the common denominator is not zero.

In the study of projective transformations it is very convenient to use the homogenous co-ordinates, i.e. in place of the three point co-ordinates we use four quantities x,y,z,w defined by the equations:

$$X = \frac{x}{w} \qquad Y = \frac{y}{w} \qquad Z = \frac{z}{w}$$

HOMOGENOUS CO-ORDINATES

Referring to figure B.1, two-dimensional (2D) space - a plane E is initially considered. An equivalent would be an x-ray picture plane in which each image point has rectangular co-ordinates X,Y.

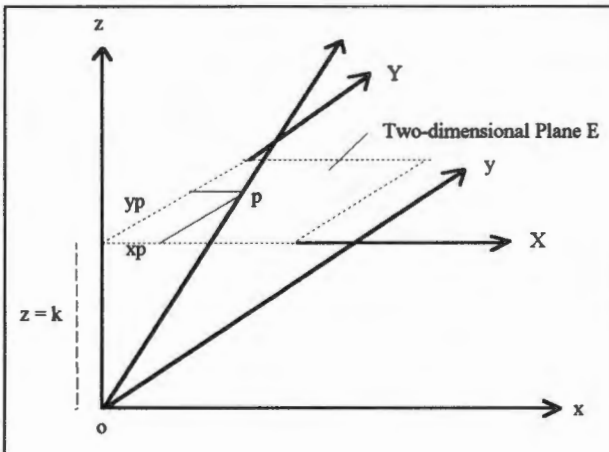

Figure B.1. A diagrammatic representation of the homogeneous co-ordinates for two-dimensional space

In plane E point P has co-ordinates X,Y in two dimensions. We now interpret x,y,z as rectangular co-ordinates in a space in which we chose the plane $z = k$ parallel to the x,y plane as the plane E. If we now join the point X,Y of E to O by a straight line then for the points on this line $\frac{x}{z}$ and $\frac{y}{z}$ are constant. If we make $z = k = 1$ we may write

$$\frac{x}{z} = X \qquad \frac{y}{z} = Y$$

Accordingly the introduction of homogenous co-ordinates signifies the representation of plane E into that space pencil of rays with origin O as centre of which E is a section.

That is, the homogeneous co-ordinates of a point are the space co-ordinates of the points of the projecting ray of that point.

The example given represents the introduction of homogeneous co-ordinates into 2-D space as for example the x-ray picture. We can form similar representation if we introduce homogeneous co-ordinates into 3-D space, that is, we think of the space as a section of $w = 1$ of a 4-D auxiliary space and we relate it to the space pencil which projects it from

the origin of auxiliary space. In this the use of 4-D space is only a convenient means of expression.

In terms of homogeneous co-ordinates equation 1 can be expressed as:

$$\begin{pmatrix} x' \\ y' \\ z' \\ w' \end{pmatrix} = A \begin{pmatrix} x \\ y \\ z \\ w \end{pmatrix} \qquad (2)$$

where matrix A is non singular.

When the accented and unaccented co-ordinates are referred to the same system, equations 1 and 2 represent a linear mapping of space onto itself which is known as collineation-non singular since A is non-singular.

In the case of x-ray pictures a difference occurs in that a singular transformation is introduced, as, to distinct planes in space there corresponds one, and only one, plane, the picture plane (fig.B.2). Such a transformation cannot be uniquely inverted for to every picture point there corresponds an infinity of space points.

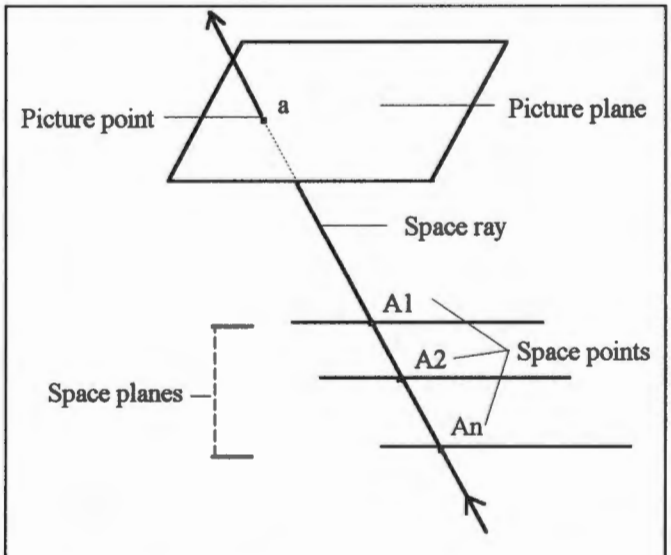

Figure B.2. An illustration of a singular transformation

HOMOGENEOUS CO-ORDINATES FOR X-RAY PICTURES

It has been shown that 2-D co-ordinates X,Y could be expressed as homogeneous co-ordinates referred to an origin O in which the point X,Y fell on a space ray projection f from O such that, for points on the ray, $\frac{x}{z} = X$ and $\frac{y}{z} = Y$ are constant.

The position of the plane containing the co-ordinated point X,Y from the origin O is therefore arbitrary but, in terms of the x-ray apparatus O is the perspective centre (assumed point focus) and $z = k$ is the perpendicular distance from the perspective centre to the plane of the film or the principal distance in photogrammetric terms.

The collinearity equation 1 is in terms of X', Y', and Z' but, for the 2-D co-ordinates x, and y and using homogeneous co-ordinates X', Y', and Z', we have

$x = \frac{X'}{Z'}$, $y = \frac{Y'}{Z'}$, where the xy plane is parallel to the $X'Y'$ plane and Z' is arbitrary and constant.

From equation 1

$$x = \frac{X'}{Z'} = \frac{a_{11}X + a_{12}Y + a_{13}Z + a_{14}}{a_{41}X + a_{42}Y + a_{43}Z + a_{44}} \times \frac{a_{41}X + a_{42}Y + a_{43}Z + a_{44}}{a_{31}X + a_{32}Y + a_{33}Z + a_{34}}$$

therefore

$$x = \frac{a_{11}X + a_{12}Y + a_{13}Z + a_{14}}{a_{31}X + a_{32}Y + a_{33}Z + a_{34}}$$

Similarly:

$$y = \frac{a_{21}X + a_{22}Y + a_{23}Z + a_{24}}{a_{31}X + a_{32}Y + a_{33}Z + a_{34}}$$

which is a convenient way of expressing x and y (the plane co-ordinates) in terms of X,Y and Z (the space co-ordinates) when we consider the x-ray case.

We can eliminate one of the transformation parameters (a_{34}) by dividing all terms on the right hand side of the equations by a_{34} and introducing new transformation parameters b_{ij} where $b_{ij} = \frac{a_{ij}}{a_{34}}$ so that we now may write:

$$x = \frac{b_{11}X + b_{12}Y + b_{13}Z + b_{14}}{b_{31}X + b_{32}Y + b_{33}Z + 1}$$

(3)

$$y = \frac{b_{21}X + b_{22}Y + b_{23}Z + b_{24}}{b_{31}X + b_{32}Y + b_{33}Z + 1}$$

DERIVATION OF SPACE CO-ORDINATES FROM PLATE CO-ORDINATES

Rewriting equation 3 and gathering terms:

$$b_{11}X + b_{12}Y + b_{13}Z + b_{14} - b_{31}xX - b_{32}xY - b_{33}xZ = x \qquad (4)$$

Similarly :

$$b_{21}X + b_{22}Y + b_{23}Z + b_{24} - b_{31}yX - b_{32}yY - b_{33}yZ = y \qquad (5)$$

Now provided sufficient control points are available, suitably distributed and co-ordinated in terms of the space X,Y,Z system and comparator (x,y) co-ordinates of their image

points in the plane of the x-ray are measured, solutions may be set up in the form of equations 4 and 5 and hence the transformation parameters b_{ij} may be solved.

Two pictures from different views provide sufficient information to solve for two different sets of b_{ij} terms, i.e. b_{ij} and $\bar{b}_{ij}$ and therefore from measurements of x,y and $\bar{x},\bar{y}$ it is possible to solve for X,Y,Z of a new point by back substitution.

From equations 4 and 5:

$$(b_{11}-xb_{31})X+(b_{12}-xb_{32})Y+(b_{13}-xb_{33})Z+b_{14}=x$$

$$(b_{21}-yb_{31})X+(b_{22}-yb_{32})Y+(b_{23}-yb_{33})Z=y \qquad (6)$$

$$(\bar{b}_{11}-\bar{x}\bar{b}_{31})X+(\bar{b}_{12}-\bar{x}\bar{b}_{32})Y+(\bar{b}_{13}-\bar{x}\bar{b}_{33})Z+\bar{b}_{14}=\bar{x}$$

$$(\bar{b}_{21}-\bar{y}\bar{b}_{31})X+(\bar{b}_{22}-\bar{y}\bar{b}_{32})Y+(\bar{b}_{23}-\bar{y}\bar{b}_{33})Z=\bar{y}$$

where the unbarred elements refer to the left hand x-ray and the barred elements refer to the right hand x-ray.

SOLUTION OF EQUATIONS

Once the b_{ij} terms have been solved the remaining calculations are straight-forward. Equations 4 and 5, however, are non-linear functions involving the b_{ij} parameters and the methods to be adopted to solve the equations are debatable. Initial values for the parameters can be determined if there are at least six control points imaged on an x-ray, but with the following restrictions:

if using the minimum of six control points, giving one redundancy, then,

i) no more than four space points should be co-planar; and

ii) no more than three images should be collinear.

Various "least squares" iterative solutions to the problem have been suggested in which space control co-ordinates are assumed error free and the comparator co-ordinates assumed subject to errors of observation, a somewhat debatable point since for very short-range photogrammetry the comparator observations are probably determined to a higher degree of accuracy than the space determinations. It seems sensible therefore to assume that both the object and image co-ordinates are error free and to solve for mean "b_{ij}" values using normal equations formed from "quasi"-observation equations as follows:

b_{11}	b_{12}	b_{13}	b_{14}	b_{21}	b_{22}	b_{23}	b_{24}	b_{31}	b_{32}	b_{33}	$= l$
X_1	Y_1	Z_1	1	0	0	0	0	$-x_1 X_1$	$-x_1 Y_1$	$-x_1 Z_1$	x_1
X_2	Y_2	Z_2	1	0	0	0	0	$-x_2 X_2$	$-x_2 Y_2$	$-x_2 Z_2$	x_2
:								:			:
X_n	Y_n	Z_n	1	0	0	0	0	$-x_n X_n$	$-x_n Y_n$	$-x_n Z_n$	x_n
0	0	0	0	X	Y	Z	1	$-y_1 X_1$	$-y_1 Y_1$	$-y_1 Z_1$	y_1
0	0	0	0	X_2	Y_2	Z_2	1	$-y_2 X_2$	$-y_2 Y_2$	$-y_2 Z_2$	y_2
:								:			:
0	0	0	0	X_n	Y_n	Z_n	1	$-y_n X_n$	$-y_n Y_n$	$-y_n Z_n$	y_n

'A' matrix

'L' matrix

From these "quasi" observation equations the "**b**" matrix can be solved from:

$$B = \left(A^T A\right)^{-1} A^T L$$

Substitution of the calculated b_{ij} and $\overline{b}_{ij}$ values and observed comparator values for image points into equation 6 leads to four solution equations for three unknowns (X,Y,Z) in the form:

X	Y	Z	$=1$
C_{11}	C_{12}	C_{13}	L_1
C_{21}	C_{22}	C_{23}	L_2
C_{31}	C_{32}	C_{33}	L_3
C_{41}	C_{42}	C_{43}	L_4

C matrix **L** matrix

where, for example,

$$C_{11} = (b_{11} - xb_{31}), \quad L_1 = (x - b_{14}) etc.$$

and X,Y,Z are the space co-ordinates of the image point which is to be co-ordinated.

In matrix notation the solution is given by:

$$\begin{pmatrix} X \\ Y \\ Z \end{pmatrix} = (C^T C)^{-1} C^T L.$$

APPENDIX C
BEAD PLACEMENTS

GENERAL PLACEMENTS

The beads used in orthopaedic applications are usually Tantalum or Vitallium balls between 0.8 mm and 1.0 mm in diameter. Tantalum has an atomic number of 73 and is thus highly visible on an x-ray. Tantalum beads with a diameter of 0.8 mm are used in the Lund system in Sweden, whereas stainless steel beads with a diameter of 1.0 mm are used in the Oxford system. Implantation of the beads takes place during surgery with as little alterations to the surgical procedure as possible. The region or general area is a more important consideration than the specific site. The regions around the greater and lesser trochanter are the most common areas for the placement of the beads. Chafetz et al (1984,1985) and Kärrholm (1989) placed beads in the above mentioned regions only. Hunter et al (1979), however, placed a bead in the shaft of the femur near the tip of the prosthesis.

SPECIFIC PLACEMENTS

Hunter et al (1979) did a study on the cemented total hip arthroplasties. Three metallic beads were implanted around the femoral component during the setting of the cement (fig.C.1). In this system three beads were all that were needed to define the plane. One bead was placed in the region of the greater trochanter and a second bead in the region of the lesser trochanter. A third bead was placed laterally along side the stem of the prosthesis in the distal fifth of the prosthetic length.

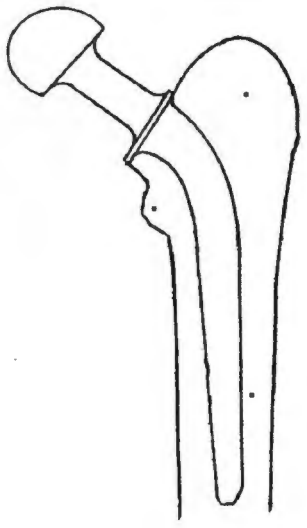

Figure C.1. A diagrammatic representation of the bead placement described by Hunter *et al.* (1979).

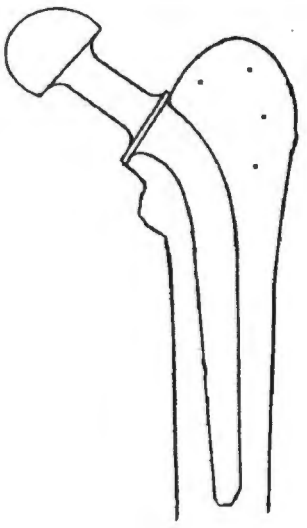

Figure C.2. A diagrammatic representation of the bead placement described by Chafetz (1984).

In 1984 Chafetz *et al.* reported a study in which four beads were placed in the region of the greater trochanter (fig. C.2). The beads were spaced as far apart as possible to avoid being obscured.

In a similar study in 1985 Chafetz *et al.* implanted three Vitallium beads with a diameter of 0.8 mm (fig.C.3). One bead was placed in the lesser trochanter and the remaining two beads were placed as far apart as possible in the greater trochanter.

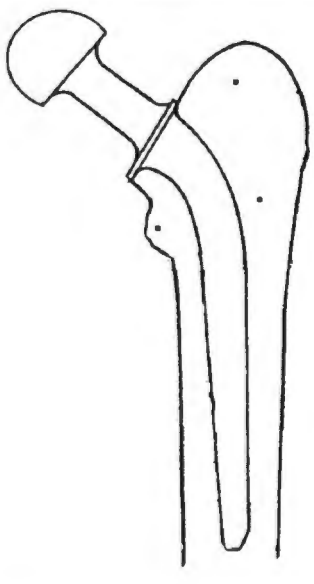

Figure C.3. The bead placement used by Chafetz *et al.* (1985).

Djerf (1987) describes a bead placement similar to that of Hunter (1979). Three Tantalum beads with a diameter of 1.0 mm were placed in holes drilled in the femur and secured with

bone cement. Single beads were placed in each of the trochanteric regions and the third bead was placed on the lateral side of the prosthesis approximately 15 cm below the greater trochanter.

Kärrholm (1989) reports on the method used in Sweden in which up to ten beads are placed in the trochanteric regions (fig.C.4). Tantalum beads with a diameter of 0.8mm were used. The minimum number of beads required for this system is five well spaced beads.

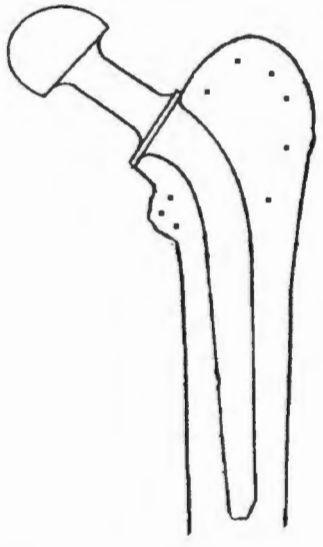

Figure C.4. Bead placement according to Kärrrholm (1989)

INSERTION METHODS

Kärrholm (1989) investigates the use of a spring-loaded piston instrument as a method to place the beads. This instrument was described by Aronson et al (1974). The beads are positioned through the soft tissue of the patient using the specially designed instrument. A local anaesthetic is applied to the area after which the needle is forced into the bone through the tissue. The depth of the needle is controlled fluoroscopically. At the required depth the Tantalum bead or pin is released, and the needle removed.

Lippert et al (1982) position the 1.0 mm stainless steel beads by means of holes, 1.5 mm deep, drilled into the bone through a cannula. The bead is dropped into the prepared hole and forced into the bone by a stylet.

Turner-Smith (1990) mentions the use of an alignment device to assist in the pattern of placement of the beads. As with the other systems the beads have to be as far apart as possible to ensure as accurate a determination of their orientation as possible.

REQUIREMENTS FOR THE SYSTEM USED IN THIS STUDY

* A minimum of four beads to ensure the accuracy of the system.

* Six beads placed around the prosthesis should be sufficient to ensure the necessary four beads are not obscured by the prosthesis in the x-ray.

* The beads should be positioned away from any metal added during the surgical procedure eg. cables and crimp sleeves.

* The beads should be as far apart as possible and as far from the prosthesis as possible to prevent the prosthesis from obscuring the beads.

* A bead placed in the area of the tip would be beneficial for detecting anterior-posterior movement of the tip with greater accuracy.

SUGGESTED PLACEMENTS

Two or three beads placed in the greater trochanteric region, below the osteotomy site

Two or three beads in the lesser trochanteric region

One or two bead on the lateral or medial the femur.

A diagram of the suggested placements is given in fig.C.7.

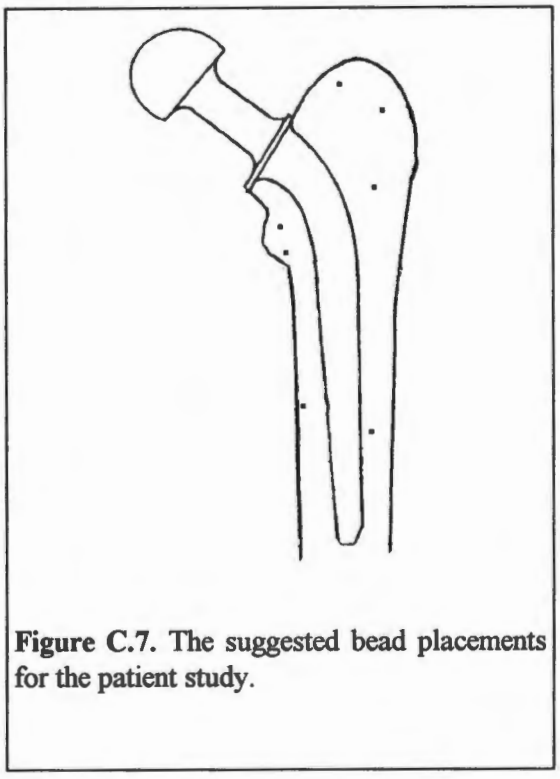

Figure C.7. The suggested bead placements for the patient study.

APPENDIX D

A "PATIENT VIDEO IMAGE"

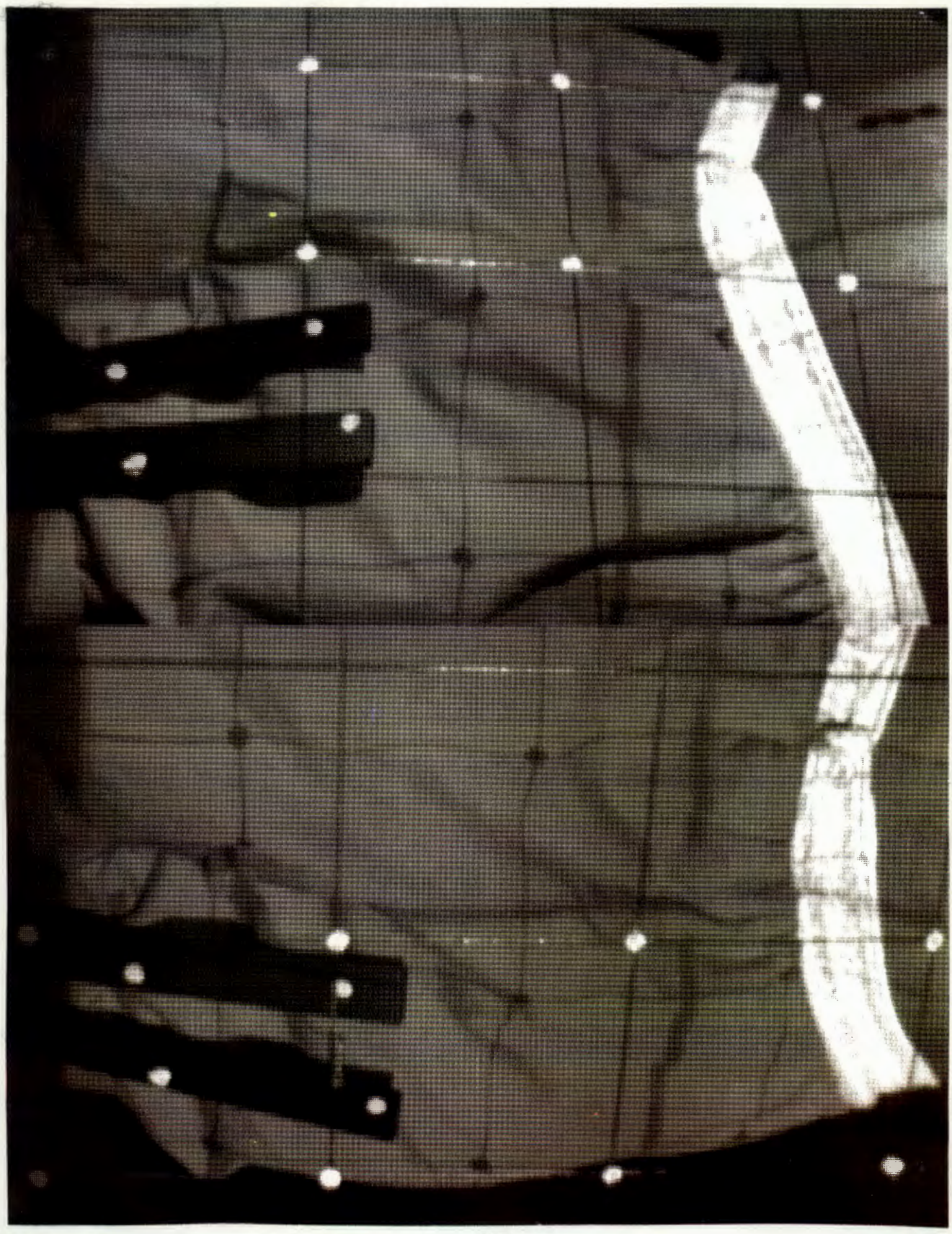

APPENDIX E

A SCHEMATIC REPRESENTATION OF THE SYSTEM SET-UP